DNA methylation as a contributor to dysregulation of *STX6* and other frontotemporal lobar degeneration genetic risk-associated loci

Naiomi Rambarack[1], Katherine Fodder[1], Megha Murthy[2], Christina Toomey[2,3], Rohan de Silva[2,4], Peter Heutink[5], Jack Humphrey[6], Towfique Raj[6], Tammaryn Lashley[1], Conceição Bettencourt[1*]

1. Department of Neurodegenerative Disease, UCL Queen Square Institute of Neurology, London, UK
2. Department of Clinical and Movement Neurosciences, UCL Queen Square Institute of Neurology, London, UK
3. The Francis Crick Institute, London, UK
4. Reta Lila Weston Institute, UCL Queen Square Institute of Neurology, London, UK
5. German Center for Neurodegenerative Diseases, Tübingen, Germany
6. Nash Family Department of Neuroscience and Friedman Brain Institute, Icahn School of Medicine at Mount Sinai, New York, NY USA

*Corresponding Author:
Conceição Bettencourt, PhD
Department of Neurodegenerative Disease
UCL Queen Square Institute of Neurology

1 Wakefield Street
London WC1N 1PJ
United Kingdom

Email c.bettencourt@ucl.ac.uk

Abstract

Frontotemporal lobar degeneration (FTLD) represents a spectrum of clinically, genetically, and pathologically heterogeneous neurodegenerative disorders. The two major FTLD pathological subgroups are FTLD-TDP and FTLD-tau. While the majority of FTLD cases are sporadic, heterogeneity also exists within the familial cases, typically involving mutations in *MAPT, GRN* or *C9orf72,* which is not fully explained by known genetic mechanisms. We sought to address this gap by investigating the effect of epigenetic modifications, specifically DNA methylation variation, on genes associated with FTLD genetic risk in different FTLD subtypes. We used frontal cortex DNA methylation profiles from three FTLD datasets containing different subtypes of FTLD-TDP and FTLD-tau: FTLD1m (N = 23) containing FTLD-TDP *C9orf72* mutation carriers and sporadic cases, FTLD2m (N = 48) containing FTLD-Tau *MAPT* mutation carriers, FTLD-TDP *GRN* and *C9orf72* mutation carriers, and FTLD3m (N = 163) sporadic FTLD-Tau (progressive supranuclear palsy - PSP) cases, and corresponding controls. We then leveraged FTLD transcriptomic and proteomic datasets to investigate possible downstream effects of DNA methylation changes. Our analysis revealed shared promoter region hypomethylation in *STX6* across FTLD-TDP and FTLD-tau subtypes, though the largest effect size was observed in PSP cases compared to controls (delta-beta = -32%, FDR adjusted-*p* value=0.002). We also observed dysregulation of the *STX6* gene and protein expression in some FTLD subtypes. Additionally, we performed a detailed examination of *MAPT*, *GRN* and *C9orf72* across subtypes and observed nominally significant differentially methylated CpGs in variable positions across the genes, often with unique patterns and downstream changes in gene/protein expression in mutation carriers. We highlight aberrant DNA methylation at different CpG sites mapping to genes previously associated with genetic risk of FTLD, including *STX6*. Our findings support convergence of genetic and epigenetic factors towards disruption of risk loci, bringing new insights into the contribution of these mechanisms to FTLD.

Keywords: Frontotemporal lobar degeneration, Frontotemporal dementia, Progressive supranuclear palsy, DNA methylation, Epigenetics, Neurodegeneration, disease risk

Introduction

Frontotemporal lobar degeneration (FTLD) represents a spectrum of clinically, genetically, and pathologically heterogeneous neurodegenerative disorders characterised by progressive atrophy of the frontal and temporal lobes of the brain (1,2). FTLD is the umbrella term that describes the neuropathology of frontotemporal dementias (FTD) and related disorders. FTD is the second most common form of early-onset dementia and FTD also represents an estimated 25% of dementia cases occurring in individuals over 65 (3,4). Damage to frontal and temporal regions of the brain typically manifests as executive dysfunction, changes in personality and behaviour and language deficits within the clinical subtypes of FTD; behavioural variant frontotemporal dementia (bvFTD), logopenic variant primary progressive aphasia (lvPPA), semantic variant PPA (svPPA)/semantic dementia (SD), nonfluent variant or progressive nonfluent aphasia (PNFA) (5). Amyotrophic lateral sclerosis (ALS) and atypical parkinsonian syndromes, including progressive supranuclear palsy (PSP), frontotemporal dementia and parkinsonism linked to chromosome 17 (FTDP-17) and corticobasal degeneration (CBD), overlap with the clinical phenotypes of FTD and are also neuropathologically classed under the FTLD umbrella (6).

The neuropathological classification of FTLD is based on the presence and morphology of protein aggregates: 50% of cases are attributed to the presence of TAR DNA-binding protein (TDP-43) positive aggregates (FTLD-TDP) (which is further divided A-E subtypes according to the genetic contribution and distribution of the aggregates), 40% to neuronal and glial inclusions of tau (FTLD-tau), while the remaining 10% is comprised of cases with inclusion bodies showing immunoreactivity for fused in sarcoma (FTLD-FUS) and FTLD-UPS involving protein inclusions of the ubiquitin proteasome system in individuals affected by a mutation in *CHMP2B*. A minority of cases show no known proteinaceous inclusions and are classified as FTLD-ni (2).

FTLD is reported to have a strong genetic component, with 30-50% of cases having a positive family history with at least one affected close relative (7). Heritability varies greatly between syndromes, with frequency of mutations also different between geographical populations (8). Most of the heritability in European populations is attributed to autosomal dominant mutations in three genes: Chromosome 9 open reading frame 72 (*C9orf72*), progranulin (*GRN*), and microtubule-associated protein tau (*MAPT*) (9–12). Rare mutations in other genes, including *TARDBP*, *VCP* and *TBK1,* have also been associated with inherited forms of FTLD (13). However, many FTLD cases are sporadic, and several genetic risk factors have been identified through genome-wide association studies (GWAS) (14–18). Single nucleotide polymorphisms (SNPs) in *MAPT* and *MOBP* loci have been associated with risk of FTD and PSP suggesting common genetic

denominators across subtypes of FTLD (18–20). SNPs in *STX6* and *EIF2AK3* have been reported to influence the risk of PSP, with no reported association with risk of FTD so far. Exploring the contributions of mutation carriers to the disease phenotype has been an avenue to elucidate which signatures are unique to causative genes (21–25). Although the identification of these FTLD risk genes has provided a basis for exploring pathways and mechanisms driving the pathology of these diseases, genetics on its own has not explained the clinicopathological heterogeneity of FTLD. Epigenetic modifications such as DNA methylation reflect the interplay between genetics and the environment. These modifications are regulatory mechanisms which influence gene expression without changing the underlying DNA sequence. As most human diseases, including neurodegenerative diseases, result from gene deregulation with loss or gain in their functions, epigenetic modifications influencing disease are gaining attention (26–29) .

We note that DNA methylation contributes to tight gene expression regulation, as this mechanism has been reported to contribute to changes in expression of the major FTD genes *GRN* and *C9orf72* in FTLD individuals compared to controls (30–33). There has been no conclusive evidence to link DNA methylation at *MAPT* to changes in its expression levels, despite preliminary suggestions of an effect in PSP (30–34). To further assess the relevance of DNA methylation in FTLD, we previously published an epigenome-wide association study (EWAS) meta-analysis using post-mortem frontal lobe DNA methylation profiles from three datasets comprised of different subtypes of FTLD-TDP and FTLD-tau (35). As ageing is a key risk factor for neurodegeneration, we have also investigated biological ageing in FTLD by using DNA methylation clocks (36,37). The results provided more evidence for the involvement of variable DNA methylation in FTLD pathogenesis and accelerated ageing (35,38).

For this study, we compiled a list of causal and risk genes associated with FTLD and leveraged *omics* data from available brain derived datasets. We investigated DNA methylation patterns in the FTLD genetic risk-related loci and determined whether the patterns varied across the heterogeneous FTLD subtypes. As DNA methylation plays a key role in regulating gene expression, we also investigated possible downstream dysregulation in gene and protein expression using transcriptomics and proteomics data. One of our main findings was dysregulation of DNA methylation at the Syntaxin-6 (*STX6*) locus across FTLD-TDP and FTLD-tau subtypes. We also report on DNA methylation patterns and further dysregulation with the major FTLD Mendelian loci (*C9orf72*, *GRN* and *MAPT*). Our findings highlight that loci previously associated with FTLD genetic risk can also be affected via aberrant DNA methylation.

Methods

Characterisation of post-mortem brain donors included in DNA methylation investigations

The details of the DNA methylation datasets used in this study are as previously described (35) (Fig. 1, Supplementary Table 1). The post-mortem tissues for FTLD1m (N=23) were obtained from brains donated to the Queen Square Brain Bank where the tissues are stored under a licence from the Human Tissue authority (No. 12198). The brain donation programme and protocols have been granted ethical approval for donation and research by the NRES Committee London Central. The post-mortem tissues for FTLD2m (N=48) were obtained through a Material Transfer Agreement with the Netherlands Brain Bank, as described by Menden *et al*. (39). The data used for FTLD3m (N = 163, after quality control) were made available by Weber *et al*. (40) and accessed through the Gene Expression Omnibus (GEO) database (GEO accession number GSE75704).

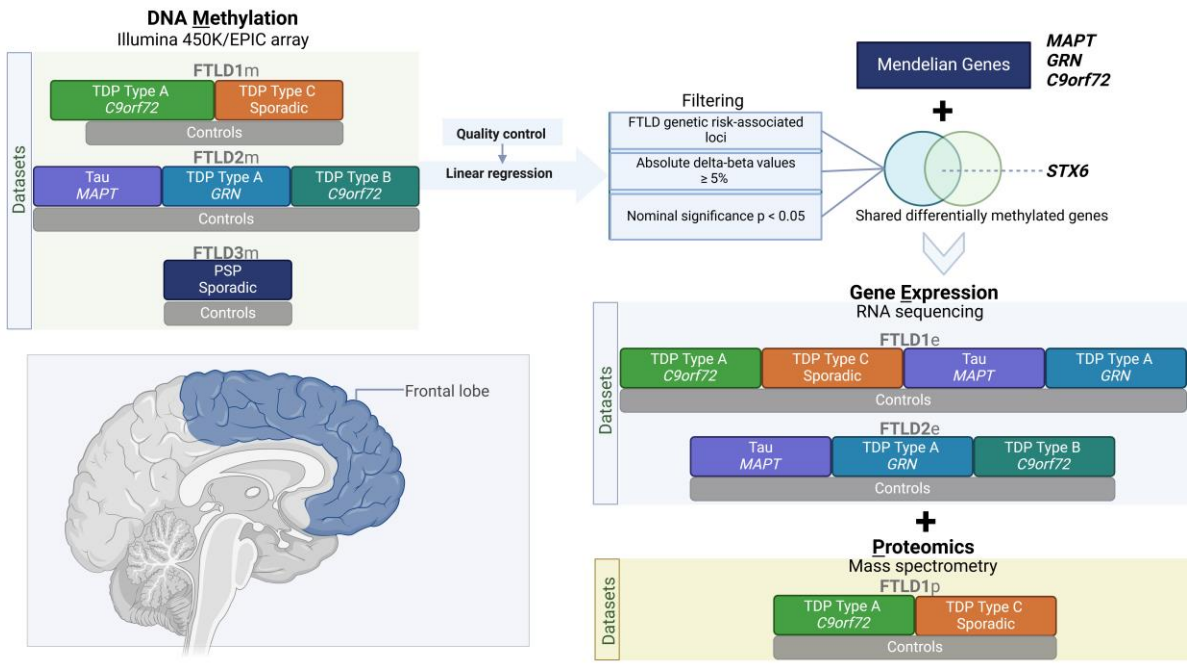

Figure 1. Overview of the study design, datasets and analysis framework. FTLD – Frontotemporal lobar degeneration, PSP – Progressive supranuclear palsy.

Compilation of known FTLD-associated loci

To focus this study on FTLD genetic risk-associated loci, we compiled a list of genes by searching the DisGeNET text-mining database by disease terms "Frontotemporal lobar degeneration" and "Progressive supranuclear palsy" alongside a literature search to validate entries to the list. Duplicated genes, those that presented with negative results and those where the findings were neither substantial nor replicated were removed. The final list of genes is shown in Supplementary Table 2.

DNA methylation patterns in FTLD-associated loci

The genome-wide DNA methylation profiles for FTLD1m (N = 23), FTLD2m (N = 48) and FTLD3m (N = 163) were generated using either the Illumina 450K or the EPIC array, as described by Fodder *et al.* (35), Menden *et al.* (39) and Weber *et al.* (40), respectively. Beta-values between 0 and 1 were used to represent the percentage of methylation at each CpG site based on the intensities of the methylated and unmethylated alleles. All analyses and quality control measures were performed using R with Bioconductor packages, as previously described (27,35). Briefly, stringent and harmonised quality control measures were performed on the three datasets through the following steps: 1. the raw data files (idat) were imported for preprocessing, 2. quality control was performed using the minfi (41), wateRmelon (42), and ChAMP (43) packages where cross-reactive probes and probes of poor quality, those mapping to common genetic variants and those mapping to X or Y chromosome, as well as samples with high failure rate (≥ 2% of probes), inappropriate clustering and mismatch of predicted and phenotypic sex, were excluded as previously reported (35). ChAMP Beta-Mixture Quantile (BMIQ) was used to normalise the beta-values which then also underwent logit transformation into M-values for further statistical analysis (44). The annotations of CpG sites mapping to FTLD-associated genes were done based on the Illumina arrays manifest files. Making use of the results from the previously conducted dataset-specific EWAS (35), we characterised in depth the FTLD-associated loci (listed in Supplementary Table 2). Further details regarding regression models used for each EWAS are described by Fodder *et al.* (35) and in Supplementary Table 1. For the current study, we have focused on all methylation sites (CpGs) mapping to FTLD-associated loci showing at least nominally significant DNA methylation changes when comparing FTLD subtypes and controls (unadjusted $p<0.05$) and an absolute delta-beta of at least 0.05 (i.e., mean difference in DNA methylation levels between cases and controls ≥5%), to ensure the reported differences/effects were biologically relevant and not due to possible technical noise. We analysed the DNA methylation patterns both across datasets and subtypes to also determine if the differential

methylation patterns were affected by the presence of certain genetic mutations. We present nominal p-values, unless otherwise specified.

Gene and protein expression patterns of FTLD-associated loci

To assess whether the expression patterns of genes associated with FTLD risk are in concert with the dysregulation of DNA methylation patterns in FTLD, we used available transcriptomics data for FTLD cases and controls. We have used gene expression data from bulk frontal cortex tissue of FTLD-TDP cases and controls (N = 44) from Hasan et *al*. (45) which has overlapping brain donors with a subset of the FTLD1 DNA methylation dataset, henceforth called FTLD1e. We also used transcriptomic data (N = 44) from the same brain donors as the FTLD2 DNA methylation dataset, called FTLD2e (39). Briefly, RNAseq data for both datasets underwent quality control and processing as previously described (45). The limma package was used to calculate normalisation factors accounting for differences in library sizes (46). Genes with low expression levels were removed i.e. genes where the maximum counts per million (CPM) value across all samples was less than 1. The voom function was used to model the mean-variance relationship and transform the counts data into log2 counts per million (log-CPM) values for linear modelling. A linear model was fitted to the transformed data used to adjust for covariates (Supplementary Table 1). For overlapping brain donors with gene expression and DNA methylation datasets, we also performed DNA methylation-gene expression correlations, using the Pearson correlation coefficient (r) with nominal p-values at a threshold of $p<0.05$.

Further to gene expression analysis, we looked at the proteomics data for the genes with the FTLD-TDP cases and controls as described in our previous study (35), also with brain donors overlapping with FTLD1 (FTLD1p), where protein levels were quantified using frontal cortex homogenate of frozen post-mortem human brain tissue on control (N = 6), FTLD-TDP type A with *C9orf72* repeat expansion (N = 6), and FTLD-TDP type C (N = 6) cases. Samples were pooled per disease group (three cases per pooled sample) to enable deeper coverage of the proteome with higher fractionation. Fold-changes and standard errors between FTLD-TDP subtypes compared to controls were calculated. As there were only two pooled samples per group, no statistical analysis was performed, but an absolute fold-change >1.5 was considered biologically meaningful. In this proteomics dataset, no data was available for some of the genes we have studied in more detail, including *GRN* and *C9orf72*.

Results

DNA methylation is dysregulated in FTLD-associated loci

This study examined in detail loci associated with the genetic risk of FTLD to determine whether these may be affected by changes in DNA methylation, possibly leading to downstream consequences on gene and/or protein expression. We leveraged frontal lobe DNA methylation data from three cohorts composed of multiple FTLD-TDP and FTLD-Tau subtypes, previously studied by Fodder *et al*. (35). The DNA methylation patterns observed for the FTLD risk genes (listed in Supplementary Table 2) showing effect sizes of at least 5% (absolute delta-betas ≥0.05) and nominal p-value <0.05, when comparing FTLD and/or its subtypes with the corresponding controls in each cohort, are shown in Figure 2 and described in Table 1. It is of note that several genes, including *MAPT,* show changes in multiple DNA methylation sites. Although DNA methylation changes are observed in promoter regions represented by CpGs mapping to TSS200 (up to 200 bases upstream of the transcription start site) and TSS1500 (200-1500 bases upstream of the transcription start site), many also occur throughout gene bodies and other regions.

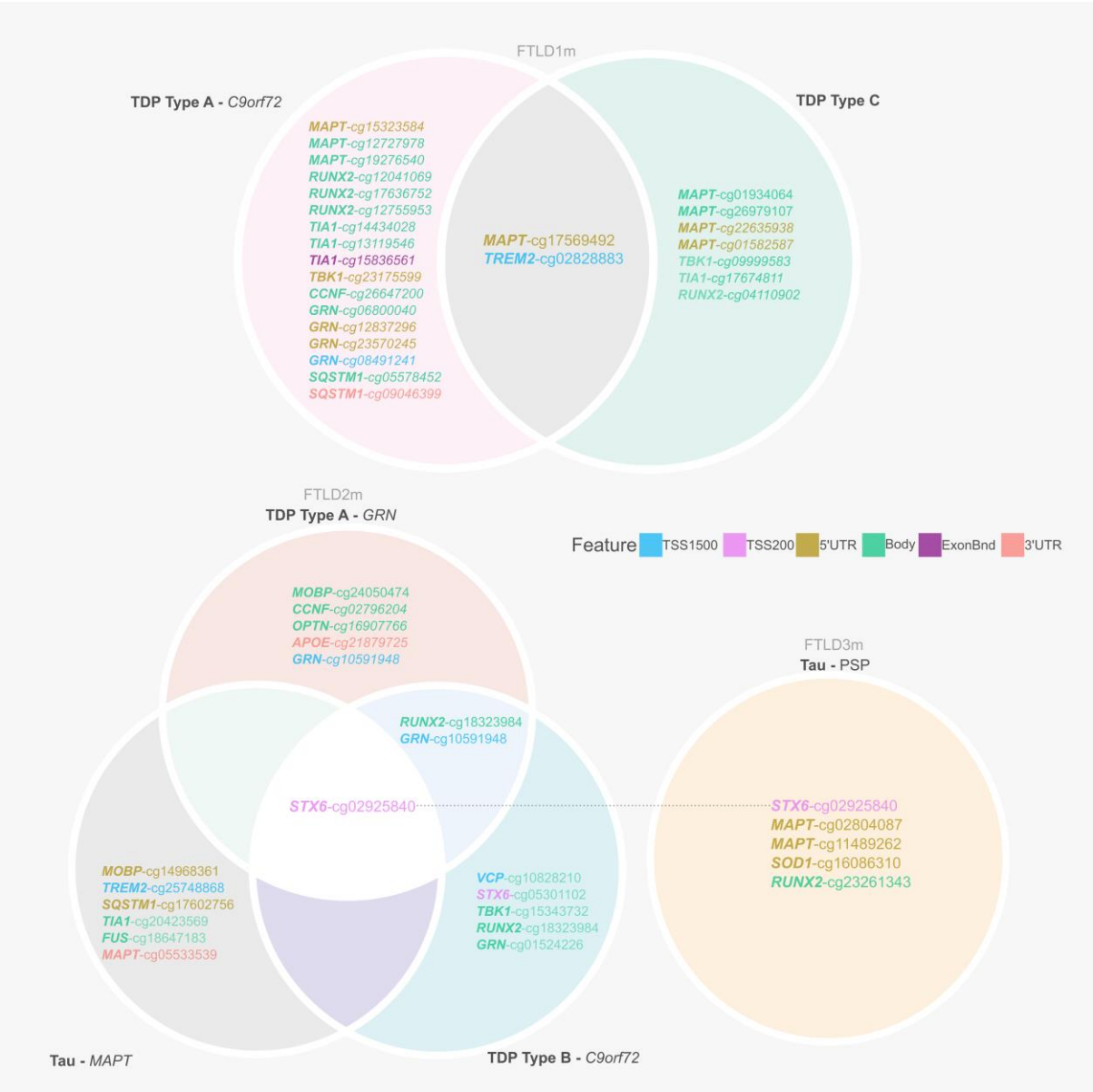

Figure 2. Overview of CpGs showing differences in DNA methylation between FTLD subtypes and controls (absolute delta-beta ≥ 5% and nominal p< 0.05) across three independent datasets (FTLD1m, FTLD2m and FTLD3m). It is of note that dysregulation of cg02925840, mapping to the promoter region of *STX6*, is shared across datasets by all FTLD2m and FTLD3m subtypes. FTLD – Frontotemporal lobar degeneration, PSP – Progressive supranuclear palsy.

Table 1: CpGs mapping to FTLD-associated loci showing differential methylation in FTLD cohorts and their subtypes compared to controls (absolute delta-beta ≥ 5% and nominal p< 0.05).

FTLD1m: FTLD vs CTRL							
Gene	**CpG**	**Chr**	**Position**	**Feature**	**CGI**	**Delta-beta**	***p*-value**
MAPT	cg01934064	17	44064242	Body	shelf	-0.14	0.024
MAPT	cg15323584	17	44022846	5'UTR	shelf	0.11	0.009
MAPT	cg17569492	17	44026659	5'UTR	island	0.09	0.019
MAPT	cg12727978	17	44075500	Body	opensea	0.08	0.009
TREM2	cg02828883	6	41131823	TSS1500	opensea	0.08	0.005
TIA1	cg14434028	2	70452453	Body	opensea	0.08	0.036
TIA1	cg13119546	2	70444039	Body	opensea	0.05	0.041
RUNX2	cg16181497	6	45409732	Body	opensea	-0.07	0.042
RUNX2	cg12755953	6	45430813	Body	opensea	0.06	0.039
RUNX2	cg04110902	6	45500999	Body	opensea	0.05	0.038
GRN	cg06800040	17	42427647	Body	shelf	0.07	0.022
FTLD1m by subtype: TDP Type A *C9orf72* vs CTRL							
MAPT	cg15323584	17	44022846	5'UTR	shelf	0.17	0.002
MAPT	cg12727978	17	44075500	Body	opensea	0.15	0.001
MAPT	cg17569492	17	44026659	5'UTR	island	0.1	0.032
MAPT	cg19276540	17	44060353	Body	island	0.08	0.035
RUNX2	cg12041069	6	45341222	Body	shelf	0.15	0.04
RUNX2	cg17636752	6	45391973	Body	shore	0.09	0.036
RUNX2	cg12755953	6	45430813	Body	opensea	0.08	0.026
TIA1	cg14434028	2	70452453	Body	opensea	0.13	0.011
TIA1	cg13119546	2	70444039	Body	opensea	0.06	0.047
TIA1	cg15836561	2	70442511	ExonBnd	opensea	0.06	0.028
TBK1	cg23175599	12	64848891	5'UTR	shelf	0.1	0.026
TREM2	cg02828883	6	41131823	TSS1500	opensea	0.09	0.017
CCNF	cg26647200	16	2482775	Body	shelf	0.09	0.022
GRN	cg06800040	17	42427647	Body	shelf	0.08	0.031
GRN	cg12837296	17	42426483	5'UTR	opensea	0.07	0.033
GRN	cg23570245	17	42426011	5'UTR	opensea	0.06	0.048
GRN	cg08491241	17	42421960	TSS1500	opensea	0.06	0.05
SQSTM1	cg05578452	5	179255653	Body	opensea	0.07	0.005
SQSTM1	cg09046399	5	179264098	3'UTR	opensea	0.06	0.025
FTLD1m by subtype: TDP Type C vs CTRL							
MAPT	cg01934064	17	44064242	Body	shelf	-0.16	0.016
MAPT	cg17569492	17	44026659	5'UTR	island	0.08	0.045
MAPT	cg26979107	17	44061355	Body	shore	0.06	0.016
MAPT	cg22635938	17	44039549	5'UTR	opensea	-0.06	0.012
MAPT	cg01582587	17	44036817	5'UTR	opensea	0.05	0.022
TBK1	cg09999583	12	64878162	Body	opensea	-0.1	0.029
TREM2	cg02828883	6	41131823	TSS1500	opensea	0.08	0.009

TIA1	cg17674811	2	70443967	Body	opensea	-0.06	0.032
RUNX2	cg04110902	6	45500999	Body	opensea	0.06	0.023
FTLD2m: FTLD vs CTRL							
TBK1	cg15343732	12	64862422	Body	opensea	0.09	0.034
STX6	cg02925840	1	180992110	TSS200	island	-0.08	0.003
MOBP	cg14968361	3	39543547	5'UTR	shore	0.08	0.050
TIA1	cg20423569	2	70452935	Body	opensea	-0.05	0.008
FTLD2m by subtype: Tau *MAPT* vs CTRL							
MOBP	cg14968361	3	39543547	5'UTR	shore	0.1	0.042
TREM2	cg25748868	6	41131213	TSS1500	opensea	0.09	0.025
SQSTM1	cg17602756	5	179246001	5'UTR	shore	-0.08	0.021
STX6	cg02925840	1	180992110	TSS200	island	-0.07	0.037
TIA1	cg20423569	2	70452935	Body	opensea	-0.06	0.005
FUS	cg18647183	16	31201691	Body	opensea	0.06	0.042
MAPT	cg05533539	17	44104521	3'UTR	opensea	0.06	0.017
FTLD2m by subtype: TDP Type A *GRN* vs CTRL							
RUNX2	cg18323984	6	45386802	Body	shore	0.09	0.018
MOBP	cg24050474	3	39544326	Body	shore	0.09	0.046
CCNF	cg02796204	16	2499223	Body	opensea	0.08	0.031
STX6	cg02925840	1	180992110	TSS200	island	-0.08	0.015
OPTN	cg16907766	10	13143470	5'UTR	shore	0.07	0.041
APOE	cg21879725	19	45412647	3'UTR	shore	-0.06	0.027
GRN	cg10591948	17	42421375	TSS1500	opensea	0.06	0.03
FTLD2m by subtype: TDP Type B *C9orf72* vs CTRL							
VCP	cg10828210	9	35072977	TSS1500	shore	-0.23	0.017
STX6	cg05301102	1	180992117	TSS200	island	-0.12	0.032
STX6	cg02925840	1	180992110	TSS200	island	-0.09	0.001
TBK1	cg15343732	12	64862422	Body	opensea	0.09	0.022
RUNX2	cg18323984	6	45386802	Body	shore	0.08	0.015
GRN	cg01524226	17	42427606	Body	shelf	0.06	0.007
GRN	cg10591948	17	42421375	TSS1500	opensea	0.06	0.03
FTLD3m: Tau PSP vs CTRL							
STX6	**cg02925840**	**1**	**180992110**	**TSS200**	**Island**	**-0.32**	**1.66E-07**
MAPT	cg02804087	17	43972969	5'UTR	Island	0.1	0.027
MAPT	cg11489262	17	43973426	5'UTR	Island	0.08	0.016
SOD1	cg16086310	21	33031992	5'UTR	Island	-0.08	0.002
RUNX2	cg23261343	6	45413792	Body	opensea	0.05	0.044

CpGs highlighted in bold reached epigenome-wide significance (FDR adjusted *p*-value ≤ 0.05). FTLD – frontotemporal lobar degeneration; PSP – progressive supranuclear palsy; CTRL – controls; CpG – DNA methylation sites; Chr – chromosome; CGI – CpG Islands and other regions; TSS – transcription start site; TSS200 – 0–200 bases upstream of TSS; TSS1500 – 200-1500 bases upstream of TSS; UTR – untranslated region.

Dysregulation in the *STX6* locus is shared across FTLD subtypes

From our analysis, one CpG mapping to the promoter region of *STX6* (cg02925840) was of particular interest, as it passed genome-wide significance in the FTLD3m dataset (FDR adjusted *p*-value = 0.002), with a strong decrease in methylation levels in the PSP cases compared to controls (delta-beta = -31.5%, Table 1, Fig. 2). Notably, *STX6* has been identified as a genetic risk locus specifically for PSP (20). Still, though to a lesser extent compared to PSP, this same CpG has shown concordant direction of effect in the FTLD2m dataset (FTLD vs controls, delta-beta = -7.9%, nominal p-value = 0.003), and in all its individual subtype comparisons (FTLD-Tau *MAPT* mutants vs controls, FTLD-TDP *C9orf72* mutants and *GRN* mutants vs controls, Table 1). An additional CpG (cg05301102) in the same region showed similar results and reached nominal significance in FTLD2m *C9orf72* mutation carriers and vs controls (delta-beta = -12%, nominal p-value = 0.032) (Fig. 3). Unfortunately, this region could not be analysed in FTLD1m, as probes were excluded during quality control pre-processing of the data (Supplementary Fig. 1). Overall, these findings suggest that disruption of DNA methylation patterns at *STX6* locus might be an important feature shared across FTLD-TDP and FTLD-tau and multiple subtypes, including *MAPT, C9orf72* and *GRN* mutation carriers, in addition to sporadic PSP.

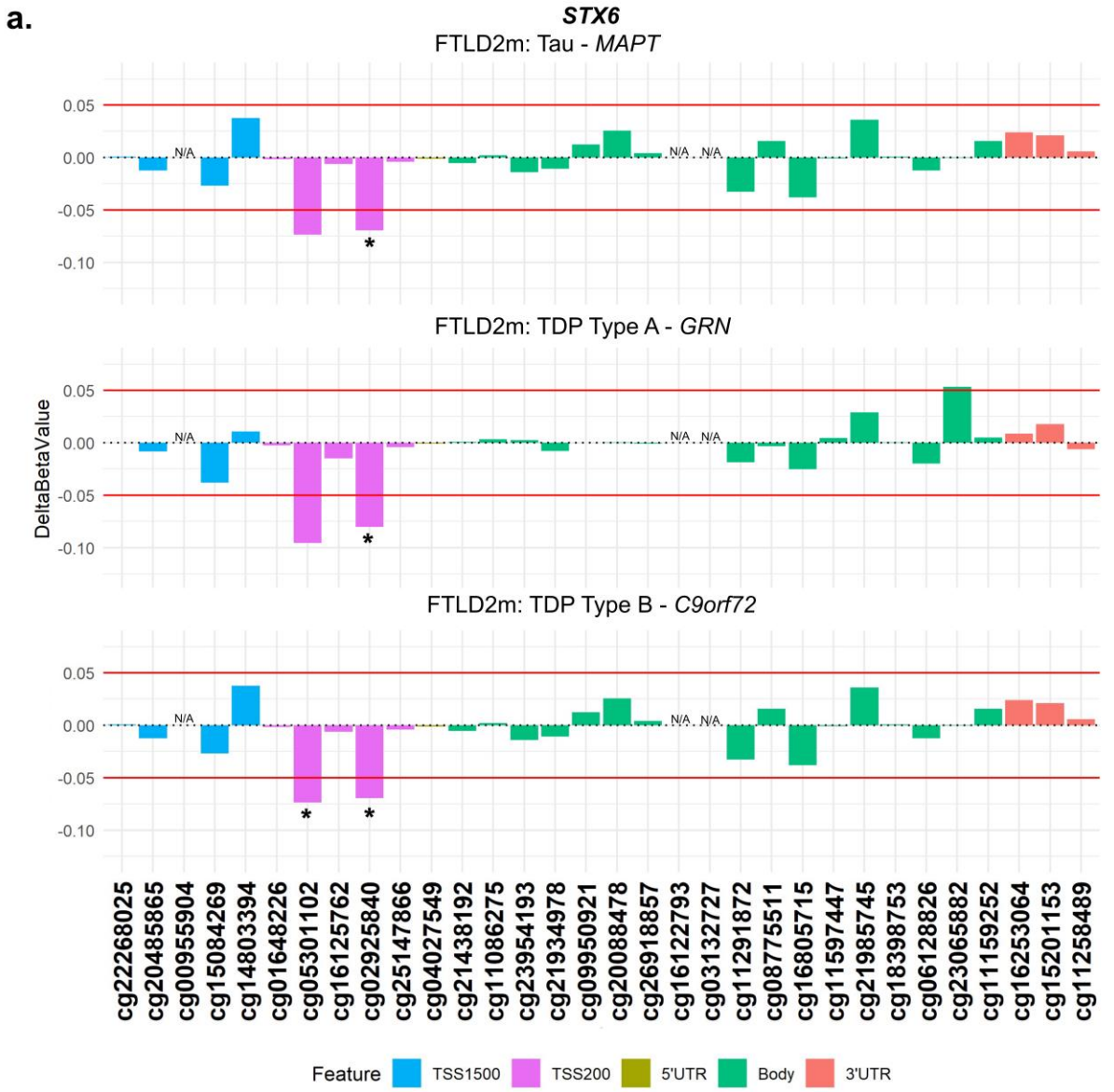
a.
STX6
FTLD2m: Tau - MAPT
FTLD2m: TDP Type A - GRN
FTLD2m: TDP Type B - C9orf72
DeltaBetaValue
0.05
0.00
-0.05
-0.10
N/A
*
cg22268025
cg20485865
cg00955904
cg15084269
cg14803394
cg01648226
cg05301102
cg16125762
cg02925840
cg25147866
cg04027549
cg21438192
cg11086275
cg23954193
cg21934978
cg09950921
cg20088478
cg26918857
cg16122793
cg03132727
cg11291872
cg08775511
cg16805715
cg11597447
cg21985745
cg18398753
cg06128826
cg23065882
cg11159252
cg16253064
cg15201153
cg11258489
Feature
TSS1500
TSS200
5'UTR
Body
3'UTR

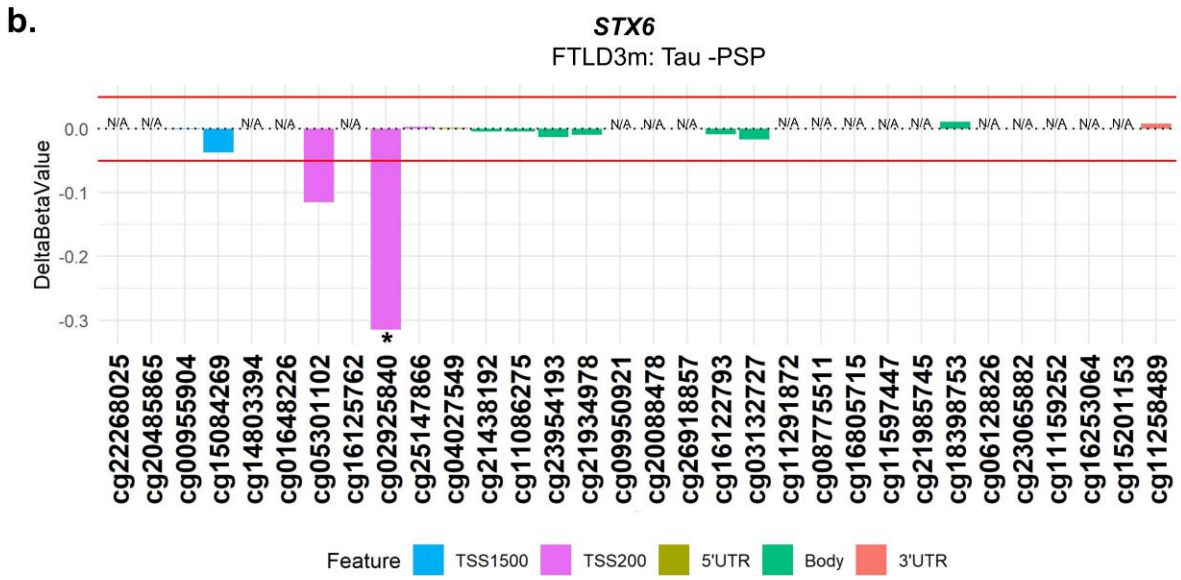
b.
STX6
FTLD3m: Tau -PSP
DeltaBetaValue
0.0
-0.1
-0.2
-0.3
N/A
*
cg22268025
cg20485865
cg00955904
cg15084269
cg14803394
cg01648226
cg05301102
cg16125762
cg02925840
cg25147866
cg04027549
cg21438192
cg11086275
cg23954193
cg21934978
cg09950921
cg20088478
cg26918857
cg16122793
cg03132727
cg11291872
cg08775511
cg16805715
cg11597447
cg21985745
cg18398753
cg06128826
cg23065882
cg11159252
cg16253064
cg15201153
cg11258489
Feature
TSS1500
TSS200
5'UTR
Body
3'UTR

Figure 3. Analysis of DNA methylation patterns across the *STX6* locus reveals that hypomethylation at the promoter region is shared across subtypes in FTLD2m and in FTLD3m (PSP). **(a)** cg02925840 in the promoter region of *STX6* is hypomethylated across subtypes of FTLD2m at the set threshold of an absolute mean difference (delta-beta value) of ≥5% represented by red horizontal lines and at least at nominal significance (*nominal $p < 0.05$). Additionally, cg05301102 also achieves nominal significance in the FTLD-TDP Type A *C9orf72* mutation carriers. **(b)** cg02925840 the promoter region of *STX6* shows strong hypomethylation in FTLD3m in PSP compared to controls (-32%) and reached epigenome-wide significance (FDR adjusted $p = 0.002$). *Indicates nominal $p < 0.05$.

FTLD2m – frontotemporal lobar degeneration DNA methylation cohort 2, FTLD3m – frontotemporal lobar degeneration DNA methylation cohort 3; PSP – progressive supranuclear palsy, TSS – transcription start site; TSS200 – 0–200 bases upstream of TSS; TSS1500 – 200-1500 bases upstream of TSS; UTR – untranslated region. *NA* – These CpGs were not available in the specified dataset due to differences in the methylation array (450K or EPIC) or removal during quality control.

Given this finding in *STX6*, we analysed available FTLD transcriptomics and proteomics datasets to investigate possible downstream consequences in gene and protein expression, respectively. Regarding gene expression (Fig. 4a,b), we observed a small increase in *STX6* expression in the FTLD1e *GRN* mutation carriers (Fold-change 1.2, nominal $p < 0.01$), only passing multiple testing corrections in FTLD sporadic TDP cases compared to controls (Fold-change 1.1, FDR adj. $p = 0.03$). We observed, however, a non-significant decrease in *STX6* expression in the *MAPT* and *C9orf72* mutation carriers represented in FTLD2e (Fold-changes -1.1, n.s.). Similarly, gene expression data analysed by Wang et al. (47), showed a non-significant decrease in *STX6* expression in PSP temporal cortex compared to controls. Leveraging a frontal cortex proteomics dataset FTLD1p, we also observed decreased STX6 protein expression in FTLD-TDP type A (*C9orf72* mutation carriers) and FTLD-TDP type C compared to controls (Fold-change -1.9 and -1.5, respectively; Fig. 4c).

Using overlapping cases between FTLD2m and FTLD2e, although non-significant, we observed a positive correlation between *STX6* expression and the top differentially methylated site - cg02925840 in the *MAPT* mutation carriers only ($r = 0.42$, n.s.; Supplementary Fig. 2), with very weak effects in all other groups. A similar direction of effect was observed for the other highlighted *STX6* CpG - cg05301102 in *MAPT* ($r = 0.20$, n.s.) as well as in *GRN* mutation carriers ($r = 0.63$, n.s.). This suggests a possible contribution of DNA methylation shaping *STX6* gene

expression landscape at least in these subtypes. However, given the small sample sizes and lack of statistical significance, these findings should be interpreted with caution and warrant further investigation.

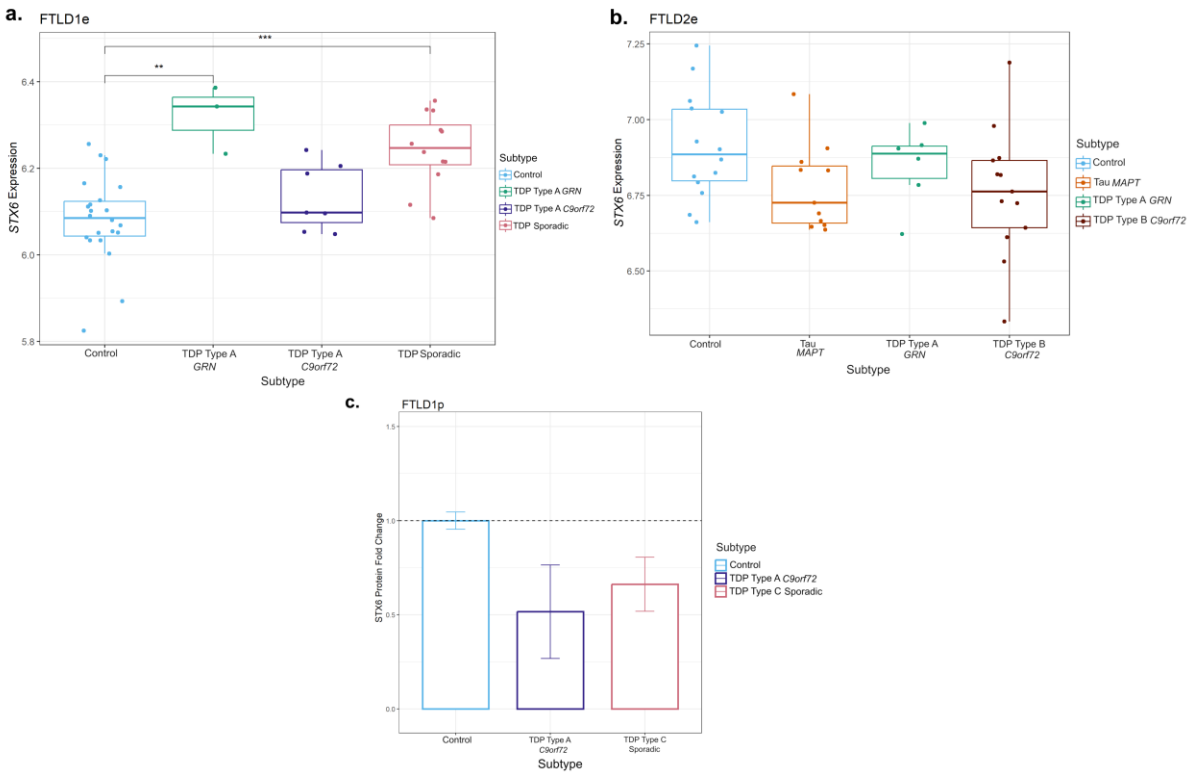

Figure 4. Gene expression and protein patterns of STX6 in frontal cortex of FTLD cases and controls. (a) Boxplot showing *STX6* gene expression in FTLD1e cases and controls, with a small increase detected in FTLD-TDP *GRN* mutation carriers and sporadic TDP cases. **(b)** Boxplot of FTLD2e showing *STX6* decreased gene expression but non-significant across all FTLD subtypes (both FTLD-TDP and FTLD-Tau) when compared to controls. Comparisons between the controls and all subtypes for the expression data were carried out using regression models adjusted for multiple covariates as detailed in Supplementary Table 1, nominal p-values are shown (**$p \leq 0.01$; ***$p \leq 0.001$). **(c)** Bar plot showing protein quantifications of STX6 in the frontal cortex of the FTLD1p dataset (FTLD TDP Type A *C9orf72* mutation carriers and FTLD TDP Type C sporadic cases). For each group we used two pooled samples (2 × 3 samples) and derived the quantifications using mass spectrometry. Both FTLD subtypes showed decreased protein expression as visualised by the fold-changes in the bar plot (TDP Type A = -1.9 and TDP Type C =-1.5); standard errors from the mean are also shown.

FTLD – frontotemporal lobar degeneration; FTLD1e – gene expression cohort 1; FTLD2e – gene expression cohort 2; FTLD1p – protein expression cohort 1.

Variable DNA methylation patterns are observed in *MAPT*, *GRN* and *C9orf72*

As mutations in *MAPT*, *GRN* and *C9orf72* represent the majority of familial FTLD cases, we used this opportunity to conduct a detailed investigation of DNA methylation patterns in these loci as well as to analyse possible downstream gene expression in both mutation carriers and non-carriers. Although *C9orf72* did not pass the set thresholds, we still included this locus in our investigation owing to its importance as a Mendelian gene.

MAPT

At the *MAPT* locus, which encodes for tau, dysregulation of DNA methylation levels was variable across FTLD datasets and subtypes, not only in FTLD-tau but also in FTLD-TDP, with several CpGs passing the thresholds of absolute delta-beta values ≥5% at nominal significance (*$p \leq 0.05$, Table 1, Fig. 5, Supplementary Fig. 3). However, the location of those above-threshold CpGs throughout the gene, seemed to differ between FTLD subtypes. The *MAPT* mutation carriers (FTLD-Tau – FTLD2m) had a unique and significantly hypermethylated CpG (cg05533539) in the 3'UTR region of the gene. While the PSP cases (FTLD-Tau – FTLD3m) had two hypermethylated CpGs (cg02804087 and cg11489262) in the 5'UTR region of the gene, none of which surpassed the chosen thresholds or same direction of effect in any other FTLD subtype. For this dataset (FTLD3m), we also stratified samples by the presence/absence of the *MAPT* H2 haplotype to explore whether it could affect DNA methylation patterns at the locus when comparing PSP with controls. However, findings for the gene were similar to those of the unstratified analysis (data not shown), suggesting the *MAPT* haplotypes are not playing a major role in the observed disease-associated DNA methylation landscape at this locus. In the FTLD1m dataset, several CpGs distributed across the gene showed variable methylation patterns, with cg01934064 and cg15323584, in the *MAPT* gene body and 5'UTR, respectively, being the topmost differentially methylated CpGs in FTLD-TDP compared to controls. However, looking at the individual subtypes within this cohort, the cg01934064 was significantly hypomethylated in the TDP type C cases (sporadic) compared to controls, while cg15323584 was hypermethylated in the TDP type A cases (*C9orf72* mutation carriers) compared to controls. The cg17569492 probe, also in the 5'UTR region, was hypermethylated in both FTLD-TDP types A and C. Further to this finding, it is of note that FTLD-TDP types A and C showed downregulation of *MAPT* protein expression compared to controls in the FTLD1p dataset (Fold-changes < -1.5, Fig. 5d). In accordance with this, in the FTLD1e expression dataset, *MAPT* expression was lower in the TDP type A *C9orf72* and sporadic TDP cases (which included TDP type C) when compared to controls (nominal $p<0.05$), while the FTLD2e dataset showed no significant differences between FTLD subtypes and controls. Wang et

al. (47) reports a non-significant increase in *MAPT* expression in PSP temporal cortex compared to controls.

Using overlapping cases between FTLD2m and FTLD2e, although non-significant, we observed a negative correlation between *MAPT* expression and the 3'UTR CpG which was hypermethylated (cg05533539) in the *MAPT* mutation carriers ($r = -0.27$, n.s.; Supplementary Fig. 4). It is of note that the controls ($r = 0.47$, $p = 0.089$) and the *C9orf72* mutation carriers showed the opposite direction of effect with positive correlations ($r = 0.53$, $p = 0.064$). Once again, these findings should be interpreted with caution due to the small sample sizes and lack of statistical significance, and warrant further investigation in future studies.

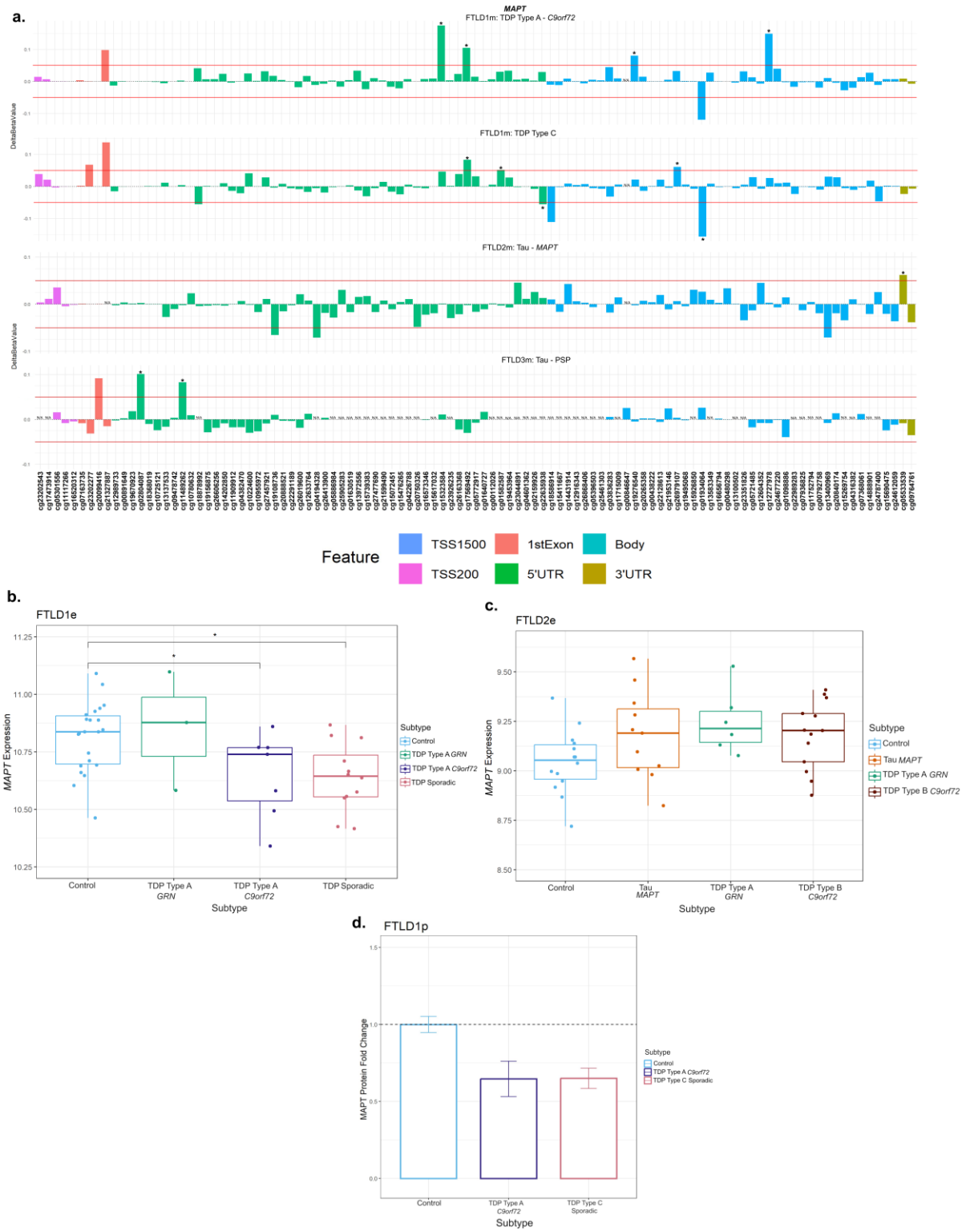

Figure 5. Mixed DNA methylation patterns in the UTRs and Body of *MAPT* with patterns of lower gene and protein expression. (a) *MAPT* mutation carriers had one hypermethylated CpG in the 3'UTR region which passed both thresholds of an absolute mean difference of ≥5% and at least at nominal significance (*nominal $p < 0.05$). Other probes surpassing these thresholds were in the 5'UTR region and the body of the gene. These showed mixed patterns of hypo- and hyper-methylation across different subtypes. **(b)** Boxplot of the FTLD1e cohort

showed lower expression of *MAPT* in all subtypes with TDP Type B *C9orf72* and sporadic TDP cases achieving significance. *Indicates $p \leq 0.05$. **(c)** Boxplot of the FTLD2e cohort showed no changes in *MAPT* expression in the subtypes. Comparisons between the controls and all subtypes for the expression data were carried out using regression models adjusted for multiple covariates as described in Supplementary Table 1. **(d)** Barplot of the FTLD1p cohort where both FTLD subtypes showed decreased protein expression as visualised by the fold-changes (TDP Type A = -1.5 and TDP Type C =-1.5); standard errors from the mean are also shown.

FTLD1e – frontotemporal lobar degeneration gene expression cohort 1; FTLD1p – frontotemporal lobar degeneration protein quantification cohort 1. TSS – transcription start site; TSS200 – 0–200 bases upstream of TSS; TSS1500 – 200-1500 bases upstream of TSS; UTR – untranslated region. *NA* – These CpGs were not available in the specified dataset due to differences in the methylation array or removal during quality control.

GRN

At the *GRN* locus we observed promoter hypermethylation in the TDP Type A cases containing different mutation carriers (FTLD1 TDP Type A – *C9orf72*, FTLD 2 TDP Type A – *GRN*) compared to corresponding controls, the CpGs cg08491241 and cg10591948, respectively, mapping to the TSS1500 region (Fig. 6a, Supplementary Fig. 5). The TDP Type A *C9orf72* subtype also showed CpGs with hypermethylation patterns in the 5'UTR and body while the TDP Type B *C9orf72* subtype had one CpG in the body surpass the set thresholds (absolute delta-beta ≥5% and nominal $p < 0.05$). In both the FTLD1e and FTLD2e datasets, when compared to controls, higher expression was observed in the *MAPT* and *C9orf72* mutation carriers while lower expression was observed in the FTLD-TDP Type A *GRN* cases in both datasets (Fold-changes of -1.2 and -1.6, respectively), as often observed with promoter hypermethylation, though this effect only achieved nominal statistical significance in FTLD2e (Fig. 6b-c).

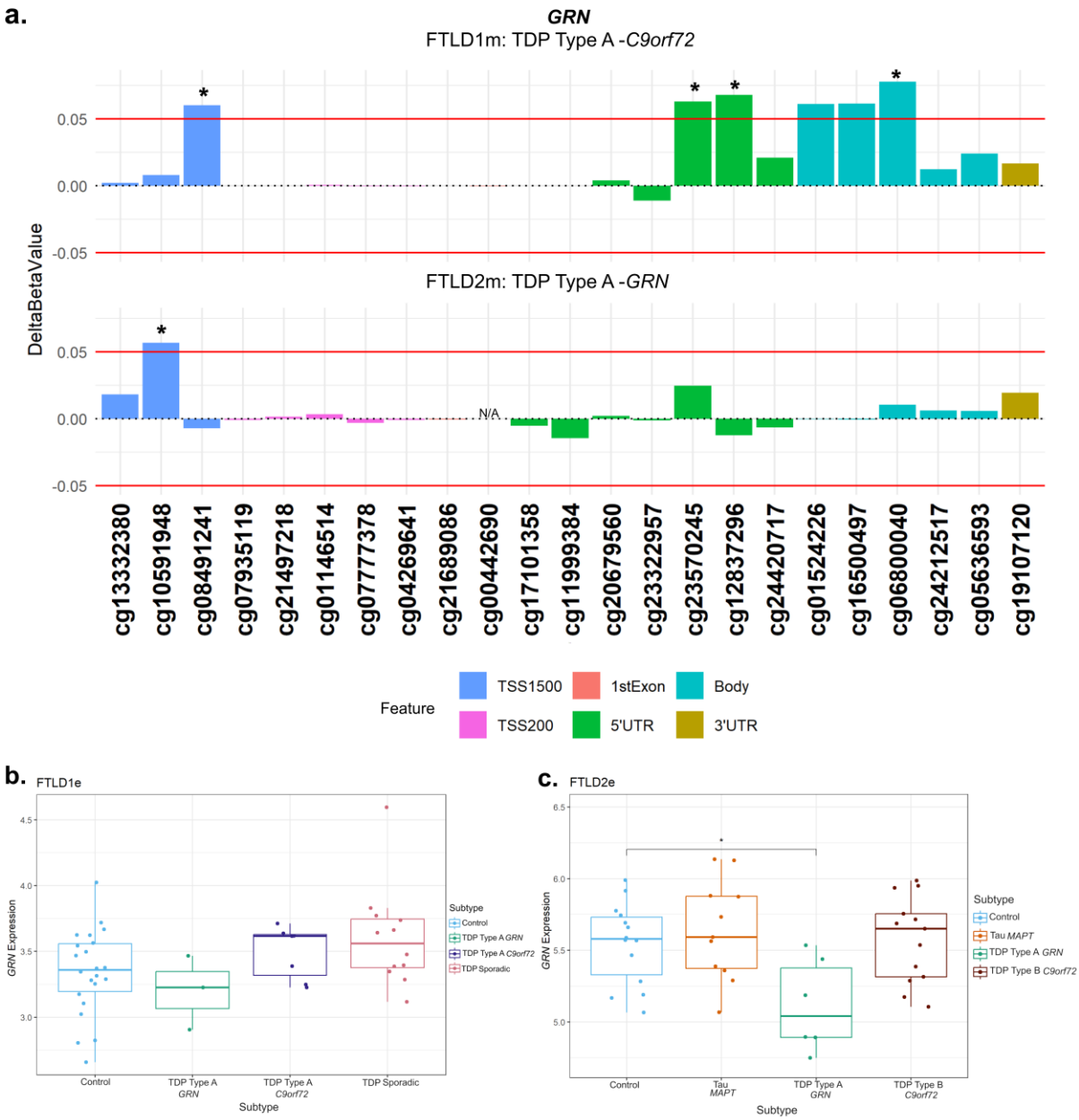

Figure 6. Promoter hypermethylation in *GRN* in FTLD-TDP Type A cases with lower gene expression in *GRN* mutation carriers. (a) The TDP Type A cases in both the FTLD1m and FTLD2m cohorts with different mutation carriers (*C9orf72* and *GRN*, respectively) showing hypermethylation in the promoter region of *GRN* passing both thresholds of an absolute mean difference of ≥5% and at least at nominal significance (nominal $p < 0.05$*). The *C9orf72* carriers also showed above-threshold hypermethylation in CpGs in the 5'UTR and gene body of *GRN*. **(b)** Boxplot of the FTLD1e cohort with mixed expression patterns of *GRN* in FTLD subtypes compared to controls with none achieving statistical significance after multiple testing corrections. **(c)** Boxplot of the FTLD2e cohort showing mixed patterns of gene expression with the FTLD-TDP Type A *GRN* mutation carriers showing a nominally significant decrease in gene expression.

Comparisons between the controls and all subtypes for the expression data were carried out using regression models adjusted for multiple covariates as described in Supplementary Table 1. *Indicates nominal $p < 0.05$. Note: the *GRN* mutation carriers were observed to show lower expression than the corresponding controls and other subtypes in both FTLD1e and FTLD2e.

FTLD1e – frontotemporal lobar degeneration gene expression cohort 1; FTLD2e – frontotemporal lobar degeneration gene expression cohort 2; TSS – transcription start site; TSS200 – 0–200 bases upstream of TSS; TSS1500 – 200-1500 bases upstream of TSS; UTR – untranslated region. *NA* – These CpGs were not available in the specified dataset due to differences in the methylation array or removal during quality control.

C9orf72

As *C9orf72* is an important gene in FTLD, even though no CpG fully met the established thresholds (absolute delta-beta ≥5% and p-value <0.05), we still detailed the DNA methylation patterns throughout the locus as well as downstream gene expression changes (Fig. 7). We observed higher DNA methylation levels with a delta-beta > 5% (n.s.) in two CpGs only in *C9orf72* mutation carriers (both the TDP Type A and TDP Type B subtypes) compared to controls (Fig. 7a, other subtypes are shown in Supplementary Fig. 4). One near the location of the *C9orf72* repeat expansion in the 5'UTR region and another within the promoter region (cg01861827 and cg14363787, respectively). We also observed a significant downregulation of *C9orf72* gene expression in *C9orf72* mutation carriers, both in FTLD-TDP types A (Fold-change = -1.3, nominal $p = 0.005$) and B (Fold-change = -1.9, FDR adj. $p = 0.003$), when compared to the corresponding controls (Fig. 7 b,c). Although to a lesser extent, decreased *C9orf72* expression was also observed in *GRN* and *MAPT* mutations carriers compared to controls, suggesting this locus may be more broadly dysregulated across FTLD subtypes.

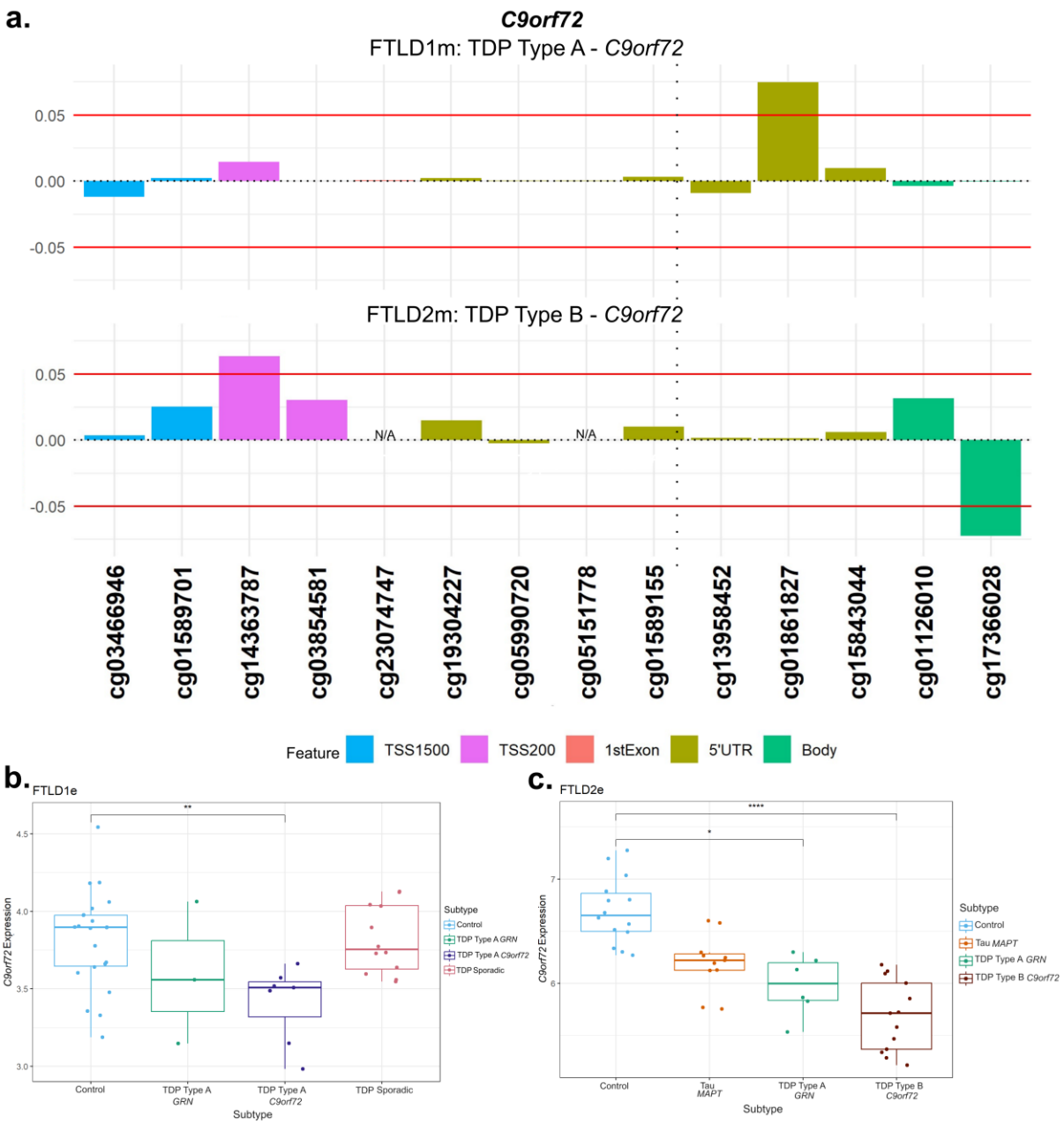

Figure 7. DNA methylation and gene expression patterns in *C9orf72*. (a) Only *C9orf72* mutation carriers (TDP Type A and TDP Type B) showed higher levels of methylation compared to the corresponding controls. The TDP Type A cases (FTLD1m) showed this effect in a CpG at the 5'UTR region while the TDP Type B cases (FTLD2m) showed the hypermethylation in a CpG at the promoter region. These CpGs passed the threshold of an absolute mean difference of ≥5% although did not achieve nominal significance (nominal p > 0.05). The vertical dotted line in the 5'UTR region represents the approximate location of the *C9orf72* G_4C_2 hexanucleotide repeat expansion. **(b)** Boxplots of the FTLD1e cohort showing lower expression of *C9orf72* all subtypes with the TDP Type A *C9orf72* mutation carriers only achieving nominal statistical significance. ** Indicates nominal $p \leq 0.01$ **(c)** Boxplots of FTLD2e where all subtypes showed lower gene expression when compared to controls with only TDP Type B *C9orf72* mutation carriers

achieving statistical significance after multiple testing corrections and TDP type A *GRN* carriers achieving nominal significance * $p \leq 0.05$; **** $p \leq 0.0001$. While all the FTLD cases showed a decrease in expression compared to controls, the *C9orf72* mutation carriers were observed to show the largest effect size.

FTLD1e – frontotemporal lobar degeneration gene expression cohort 1; FTLD2e – frontotemporal lobar degeneration gene expression cohort 2; TSS – transcription start site; TSS200 – 0–200 bases upstream of TSS; TSS1500 – 200-1500 bases upstream of TSS; UTR – untranslated region. *NA* – These CpGs were not available in the specified dataset due to differences in the methylation array or removal during quality control.

Discussion

FTLD has a strong genetic component both in terms of Mendelian genes and in genes associated with risk in sporadic cases. However, genetics alone cannot explain the clinicopathological heterogeneity and/or overlap between FTLD subtypes. This suggests that epigenetic regulatory mechanisms, such as DNA methylation, that represent the interplay between the genetic makeup of an individual and their environmental exposures, may be at play in FTLD. We therefore set up this study to investigate whether DNA methylation changes could contribute to dysregulation of known FTLD genetic risk-associated loci, and how this is affected. For this study, we used DNA methylation data derived from frontal cortex tissue of three independent cohorts, including FTLD-TDP and FTLD-tau pathology, which we had investigated previously from a different perspective (35). We also combined these datasets with overlapping or corresponding gene and protein expression datasets (35,45) to further characterise possible dysregulation of such FTLD-associated loci. Our findings highlighted DNA methylation changes in *STX6*, shared across different FTLD subtypes as a major finding. Furthermore, by characterizing DNA methylation and gene expression in known FTLD Mendelian genes (i.e., *MAPT*, *GRN* and *C9orf72*), we found that dysregulation may occur even in non-mutation carriers. To our knowledge this is the first comprehensive analysis of DNA methylation patterns and characterisation of its possible downstream consequences in FTLD-associated loci, in mutation and non-mutation carriers and in a range of FTLD-TDP and FTLD-tau subtypes.

The "DNA methylation paradox" underscores the complex relationship between DNA methylation and gene expression. Promoter DNA methylation has garnered attention owing to a typically inverse correlation with gene expression (48–53). Similarly, DNA methylation in the 5' untranslated region (UTR) has been inversely correlated with gene expression, while in the 3' UTR

region a positive correlation has been observed (53–55). Our analysis highlighted two hypomethylated CpGs at the promoter region of *STX6* (cg05301102 and cg02925840) in multiple genetic forms of FTLD (all subtypes of FTLD2m, including *MAPT*, *GRN* and *C9orf72* mutation carriers) and in sporadic PSP (FTLD3m), with a much larger effect size in the latter. Interestingly, genetic variants in *STX6* had been significantly associated with risk of PSP (FTLD-tau) in multiple studies (20,56–58). *STX6* encodes syntaxin 6, which is a soluble N-ethylmaleimide sensitive factor attachment protein receptor (SNARE)-class protein involved in regulation of vesicle membrane fusion (59). Although syntaxin 6 is widely expressed in tissues throughout the body, Bock, Lin and Scheller showed in their seminal work that the brain is among the tissues expressing the highest levels of STX6 protein (60). Dysregulation of STX6 expression has been associated with AD risk and faster cognitive decline potentially relating to neuronal circuitry pathways (61,62). It has also been associated with PSP risk, as more specifically the SNP rs1411478 risk allele has been associated with decreased *STX6* expression levels in the white matter (56). Variants in and around *STX6* have also been associated with risk of the prion disease, specifically sporadic Creutzfeldt-Jakob disease, with a recent study showing that genetic upregulation of both gene and protein expression of syntaxin-6 in the brain is associated with the disease risk (63–65). Dysregulated transport of misfolded proteins from the endoplasmic reticulum to lysosomes has been hypothesized as an underlying mechanism of STX6 (20,56). Recently, an expression quantitative trait loci (eQTL) colocalization has been shown for *STX6* specifically in oligodendrocytes and brain regions associated with PSP pathology (58). DNA methylation has been implicated in the development, differentiation, and maintenance of oligodendrocyte lineage cells where *STX6* is highly expressed (58,66) therefore, its dysregulation is likely playing a role in disease. It is also of note that PSP, shows tau pathology in oligodendrocytes in the form of coiled bodies (67).

Tau is a microtubule-associated protein, encoded by the *MAPT* gene, which becomes abnormally phosphorylated leading to aggregation and formation of intracellular filamentous inclusions, consisting of hyperphosphorylated tau, in several neurodegenerative diseases. These diseases are called tauopathies and include AD as well as several diseases under the FTLD umbrella (FTLD-tau) such as PSP, Pick's disease, corticobasal degeneration (CBD), argyrophilic grain disease, and frontotemporal dementia with parkinsonism linked to chromosome 17 (FTDP-17), most of which are sporadic with the exception of the latter which is caused by mutations in *MAPT* (such as the *MAPT* mutation carriers in FTLD2m) (2,68). Interestingly, the work by Lee et al. shows a link between syntaxins 6 and 8 and tau, more specifically that they are important in mediating tau secretion through their interaction with the C-terminal tail region of tau (69). Additionally, it

has been proposed that pathological TDP-43 is spread between cells in an autophagy-dependent, prion-like manner via extracellular vesicles potentially involving STX6 (70–72). Our findings of *STX6* dysregulation across distinct pathologies supports a broader involvement of *STX6* in both FTLD-TDP and FTLD-tau subtypes.

MAPT is one of the main Mendelian genes associated with FTLD where individuals harbour autosomal dominant mutations (9,73), influencing alternative splicing patterns, producing imbalances in tau isoforms, and/or production of more aggregation-prone mutant tau protein (74–76). Common genetic variation in the *MAPT* locus is also associated with risk of FTLD-tau in non-mutation carriers (20,58,77,78). *MAPT* sits within a complex locus (79) with large insertion-deletion polymorphisms in a large region of Chromosome 17q that is in complete linkage disequilibrium, resulting in two major haplotypes, H1 and its inverted counterpart H2, as well as some sub-haplotypes (80,81). H1 is the most common haplotype and is associated with increased risk of sporadic FTLD tauopathies, mainly the four-repeat tauopathies, CBD and PSP (20,79–81), while the H2 haplotype is protective for PSP and CBD and has been associated with familial FTD and increased risk for the three-repeat tauopathy, Pick's Disease (81–83). Li et al. performed DNA methylation analysis in peripheral blood of FTLD cases, including PSP, and concluded that DNA methylation at the region of the *MAPT* locus may influence the risk of developing tauopathies alongside the H1/H2 haplotypes (84). In studies using brain tissue, *MAPT* DNA methylation patterns have been variable and region-specific as investigated in PSP, AD and Parkinson's Disease (34,85,86).

Previous studies have reported no significant differences in methylation in FTLD-spectrum cases compared to controls (30,87). However, we observed several differentially methylated CpGs at the *MAPT* gene body and UTRs in our cohorts in both FTLD-TDP and FTLD-tau subtypes. We note that while DNA methylation patterns for different CpGs at the 5'UTR were variable, all those passing the significance thresholds were hypermethylated. The *MAPT* mutation carriers had a significantly hypermethylated CpG in the 3'UTR (cg05533539), which was not observed in any of the other FTLD subtypes. We found increased expression of *MAPT* across the FTLD2e subtypes, none of which were statistically significant. On the other hand, we found decreased expression in FTLD1e type A with *C9orf72* mutation cases and in sporadic cases (including TDP type C), consistent with FTLD1p decrease in protein expression. Untranslated regions have roles in regulating gene expression (54,88,89). However, the effect of DNA methylation at these regions remains unclear. *MAPT* has a core promoter around its first exon, but it has also been suggested to have alternative promoters at different transcription start sites (76,90), which also affect the length of 3' and 5' UTRs (76,88). Taken together, the complexity of *MAPT*'s structure aligns with its

high variability in methylation and gene and protein expression in FTLD. Whether UTRs play a significant role in regulating expression in *MAPT* remains a point for future investigation. Overall, these findings also suggest that the dysregulation at the *MAPT* locus is not confined to *MAPT* mutation carriers or tau pathology, but also extends to non-mutation carriers and those with other FTLD pathologies such as FTLD-TDP.

Mutations in *GRN,* which encodes progranulin, are another major cause of autosomal dominant FTLD. These mutations result in decreased expression and loss-of-function of the mutant allele of *GRN* resulting in haploinsufficiency and reduced expression of progranulin (10,91–93). This is particularly important in a disease context as progranulin is proposed to localise near endosomes and lysosomes to participate in endocytosis, secretion and other related key functions (94–96). Additionally, progranulin is involved in neuroinflammation, axonal growth, development and acts as a neurotrophic factor promoting neuronal survival (97,98). *GRN* has also been suggested as a modifier of risk for sporadic cases of FTLD. However, this finding may be related to a disruption of lysosomal activities chaperoned by *GRN* and requires further investigation (99,100). Still, the proposed role for *GRN* across FTLD in conjunction with an appearance of asymmetric cortical atrophy specific to the mutation carriers has provided a strong argument to determine regulatory mechanisms, including epigenetic mechanisms, influencing *GRN* expression (101,102). Hypermethylation at the promoter region of *GRN* has been inversely correlated with gene expression and therefore reduced *GRN* expression in FTLD in sporadic cases (32,33). Banzhaf-Strathmann *et al.* showed hypermethylation at the promoter region in *GRN* in FTLD compared to AD and PD (33). Likewise, we have shown hypermethylation in the promoter region of *GRN* in FTLD-TDP Type A cases not only in *GRN* but also in *C9orf72* mutation carriers. We observed lower *GRN* expression in the *GRN* mutation carriers only though, possibly emphasizing the impact of genetic variation and suggesting that DNA methylation dysregulation beyond the promoter region, as seen in the *C9orf72* mutation carriers, may act differently and/or in concert with other mechanisms to regulate *GRN* gene expression.

Expansion of the non-coding G_4C_2 hexanucleotide repeat in the 5'UTR region of *C9orf72* is the most common cause of familial FTLD (8). The mechanism by which this mutation causes disease remains an area of intense research as multiple pathways have been implicated (103). Like *GRN,* haploinsufficiency with reduced *C9orf72* expression and loss-of-function has been proposed (104). Toxic gain-of-function mechanisms have also been suggested (31,105–110). The biological role of *C9orf72* also remains unclear. However, recent studies observing protein-protein interactions suggest involvement in lysosomal activity, vesicle trafficking, axon growth, regulation of mTORC1 signalling and of inflammation (111,112).

Reduced expression of *C9orf72* has been observed in some mutation carriers. Therefore, DNA methylation patterns have been previously analysed to determine whether there was a role for this reversible mechanism in regulating *C9orf72* expression in FTLD (11,31,113,114). Hypermethylation at *C9orf72* has been observed uniquely in mutation carriers in a region upstream of the repeat (115). As *C9orf72* promoter hypermethylation results in reduced *C9orf72* expression, it is suggested to be a protective mechanism acting against the toxic gain-of-function mechanisms including reducing the amount of RNA foci while also validating a loss-of-function mechanism (115). Our results showed promoter hypermethylation in FTLD-TDP type B *C9orf72* mutation carriers. *C9orf72* expression was reduced in all studied FTLD subtypes but with the largest effect size being observed in the *C9orf72* mutation carriers, both in FTLD1e and FTLD2e. This is in line with a previous study that showed reduced expression of *C9orf72* in repeat expansion mutation carriers as well as *MAPT* and *GRN* mutation carriers, and proposed that additional mechanisms independent of promoter hypermethylation, which is primarily observed in *C9orf72* mutation carriers, regulates *C9orf72* expression across FTLD subtypes (113).

As with other studies, there are several limitations. We examined patterns in DNA methylation between subtypes of FTLD, however, this meant using relatively small sample sizes to compare across subtypes which reduced the statistical power to detect additional genome-wide changes. The available DNA methylation profiles were derived using Illumina 450K/EPIC arrays, which are not comprehensive despite their coverage throughout the genome. This is particularly important for complex genes where not all regions overlap with predefined regions covered in the arrays. As DNA methylation and gene expression may vary depending on the cellular composition and properties of a sample, there may still be differences in the tissue once chipped, which may influence findings in this type of study to some degree and cannot be fully accounted for using statistical approaches. We note that even in those donors that have overlapping samples there may be some sample variability between different omics modalities. We were also limited by the lack of full overlap between samples used to generate DNA methylation and gene expression datasets to further dissect possible downstream consequences. Additionally, we cannot completely exclude the possibility that unmeasured genetic variants, including large structural variants, may have an effect on the detection of DNA methylation changes. However, leveraging available DNA methylomics, transcriptomics and proteomics datasets, we strived to report the most consistent findings, with a meaningful biological effect (e.g., absolute delta-beta ≥5% in group comparisons), and analysed the concordance with previously published studies whenever possible.

In summary, this study explored for the first time a cross-subtype analysis of the contribution of DNA methylation to the dysregulation of FTLD genetic risk loci, with or without the presence of genetic mutations in Mendelian FTLD genes. We highlight *STX6* that showed consistent hypomethylation of the promoter region across FTLD subtypes and cohorts. On that basis, our findings support a role for *STX6* in other FTLD subtypes beyond PSP. We suggest that DNA methylation may be influencing *STX6* gene expression levels, at least in some FTLD subtypes. However, it would be important to replicate and analyse this point further in future studies with larger samples sizes per subtype. Taking into consideration a role in regulation of protein localization and its complex relationship with tau, and possibly TDP-43, the role of syntaxin-6 in various subtypes of FTLD warrants further investigation. Additionally, we focused on the Mendelian genes *MAPT*, *GRN,* and *C9orf72* where we describe patterns of DNA methylation and gene expression and showed that dysregulation is not necessarily unique to mutation carriers. Understanding the mechanisms underlying the dysregulation of such genes, including DNA methylation changes, will be key to the development of therapies. Overall, our findings have shown DNA methylation changes in FTLD-associated genes across FTLD subtypes both in carriers of known genetic mutations and in sporadic cases. We highlight that such epigenetic modifications may be a shared mechanism across FTLD subtypes possibly contributing to the dysregulation of gene expression and can provide new insights into genes associated with disease.

Ethics approval and consent to participate

The post-mortem tissues used to generate the FTLD1 datasets were obtained from brains donated to the Queen Square Brain Bank, where the tissues are stored under a licence from the Human Tissue authority (No. 12198). The brain donation programme and protocols have been granted ethical approval for donation and research by the NRES Committee London Central. The post-mortem tissues used to generate the FTLD2 datasets were obtained from The Netherlands Brain Bank (NBB), Netherlands Institute for Neuroscience, Amsterdam. All NBB Material has been collected from donors for whom a written informed consent was obtained for a brain donation and the use of the material and clinical information for research purposes. The FTLD3 DNA methylation dataset was accessed through a public repository (GEO accession number GSE75704). As described by Weber *et al*. (40), the use of human brain tissue to generate that dataset had been approved by the ethics committees of the University of Giessen and of the

Technical University of Munich. All brain samples were from patients who had given informed consent before death.

Consent for publication

Not applicable.

Availability of data and materials

Raw DNA methylation and/or RNAseq data from cohorts FTLD1, FTLD2 and FTLD3 can be accessed via the European Genome-Phenome Archive (accession number EGAD00010002055, EGAD00001008014) and NCBI GEO database (accession number GSE75704, and GSE153960). Additional data is available from the corresponding author upon reasonable request.

Competing interests

The authors declare that they have no competing interests.

Funding

The FTLD2 datasets were funded in part by the EU Joint Programme - Neurodegenerative Disease Research (JPND) project: Risk and Modifying factors for FTD (RiMod-FTD) and the NOMIS Foundation (awarded to PH). NR is supported by Alzheimer's Research UK. KF is supported by the Medical Research Council (MR/N013867/1). MM is supported by the Multiple System Atrophy Trust. RdS is supported by Reta Lila Weston Trust for Medical Research and CurePSP. JH and TR are supported by NIH NINDS U54NS123743. TL is supported by Alzheimer's Society, Alzheimer's Research UK and the Association of Frontotemporal Dementia. CB is supported by Alzheimer's Research UK and the Multiple System Atrophy Trust. The funding bodies had no role in the design of the study or collection, analysis, and interpretation of data nor in writing the manuscript.

Authors' contributions

NR contributed to data analysis, prepared the figures, and drafted the manuscript; KF and MM contributed to data analysis and interpretation; CT, RdS, PH, JH, TR, TL contributed with datasets and/or interpretation; CB conceptualised and supervised the study; All authors critically reviewed and approved the manuscript.

Acknowledgements

The authors would like to thank UCL Genomics centre for processing the EPIC arrays for the for the FTLD1m cohort. The authors would also like to acknowledge the Queen Square Brain Bank (London, UK), and the Dutch Brain Bank, Netherlands Institute for Neuroscience (Amsterdam, Netherlands) for providing brain tissues from FTLD cases and controls. The Queen Square Brain Bank is supported by the Reta Lila Weston Institute of Neurological Studies, UCL Queen Square Institute of Neurology.

References

1. Neary D, Snowden JS, Gustafson L, Passant U, Stuss D, Black S, et al. Frontotemporal lobar degeneration: a consensus on clinical diagnostic criteria. Neurology. 1998 Dec;51(6):1546–54.

2. Lashley T, Rohrer JD, Mead S, Revesz T. Review: An update on clinical, genetic and pathological aspects of frontotemporal lobar degenerations. Neuropathol Appl Neurobiol. 2015;41(7):858–81.

3. Onyike CU, Diehl-Schmid J. The Epidemiology of Frontotemporal Dementia. Int Rev Psychiatry Abingdon Engl. 2013 Apr;25(2):130–7.

4. Young JJ, Lavakumar M, Tampi D, Balachandran S, Tampi RR. Frontotemporal dementia: latest evidence and clinical implications. Ther Adv Psychopharmacol. 2018 Jan;8(1):33–48.

5. Rabinovici GD, Miller BL. Frontotemporal Lobar Degeneration. CNS Drugs. 2010 May 1;24(5):375–98.

6. Lomen-Hoerth C. Characterization of amyotrophic lateral sclerosis and frontotemporal dementia. Dement Geriatr Cogn Disord. 2004;17(4):337–41.

7. Rohrer JD, Guerreiro R, Vandrovcova J, Uphill J, Reiman D, Beck J, et al. The heritability and genetics of frontotemporal lobar degeneration. Neurology. 2009 Nov 3;73(18):1451–6.

8. Greaves CV, Rohrer JD. An update on genetic frontotemporal dementia. J Neurol. 2019;266(8):2075–86.

9. Hutton M, Lendon CL, Rizzu P, Baker M, Froelich S, Houlden H, et al. Association of missense and 5'-splice-site mutations in tau with the inherited dementia FTDP-17. Nature. 1998 Jun;393(6686):702–5.

10. Baker M, Mackenzie IR, Pickering-Brown SM, Gass J, Rademakers R, Lindholm C, et al. Mutations in progranulin cause tau-negative frontotemporal dementia linked to chromosome 17. Nature. 2006 Aug;442(7105):916–9.

11. DeJesus-Hernandez M, Mackenzie IR, Boeve BF, Boxer AL, Baker M, Rutherford NJ, et al. Expanded GGGGCC Hexanucleotide Repeat in Noncoding Region of C9ORF72 Causes Chromosome 9p-Linked FTD and ALS. Neuron. 2011 Oct 20;72(2):245–56.

12. Renton AE, Majounie E, Waite A, Simón-Sánchez J, Rollinson S, Gibbs JR, et al. A Hexanucleotide Repeat Expansion in C9ORF72 Is the Cause of Chromosome 9p21-Linked ALS-FTD. Neuron. 2011 Oct 20;72(2):257–68.

13. Pottier C, Ravenscroft TA, Sanchez-Contreras M, Rademakers R. Genetics of FTLD: overview and what else we can expect from genetic studies. J Neurochem. 2016;138(S1):32–53.

14. Van Deerlin VM, Sleiman PMA, Martinez-Lage M, Chen-Plotkin A, Wang LS, Graff-Radford NR, et al. Common variants at 7p21 are associated with frontotemporal lobar degeneration with TDP-43 inclusions. Nat Genet. 2010 Mar;42(3):234–9.

15. Ferrari R, Hernandez DG, Nalls MA, Rohrer JD, Ramasamy A, Kwok JBJ, et al. Frontotemporal dementia and its subtypes: a genome-wide association study. Lancet Neurol. 2014 Jul 1;13(7):686–99.

16. Ferrari R, Grassi M, Salvi E, Borroni B, Palluzzi F, Pepe D, et al. A genome-wide screening and SNPs-to-genes approach to identify novel genetic risk factors associated with frontotemporal dementia. Neurobiol Aging. 2015 Oct 1;36(10):2904.e13-2904.e26.

17. Pottier C, Ren Y, Perkerson RB, Baker M, Jenkins GD, van Blitterswijk M, et al. Genome-wide analyses as part of the international FTLD-TDP whole-genome sequencing consortium reveals novel disease risk factors and increases support for immune dysfunction in FTLD. Acta Neuropathol (Berl). 2019 Jun 1;137(6):879–99.

18. Manzoni C, Kia DA, Ferrari R, Leonenko G, Costa B, Saba V, et al. Genome-wide analyses reveal a potential role for the MAPT, MOBP, and APOE loci in sporadic frontotemporal dementia. Am J Hum Genet. 2024 Jul 11;111(7):1316–29.

19. Hughes A, Mann D, Pickering-Brown S. Tau haplotype frequency in frontotemporal lobar degeneration and amyotrophic lateral sclerosis. Exp Neurol. 2003 May 1;181(1):12–6.

20. Höglinger GU, Melhem NM, Dickson DW, Sleiman PMA, Wang LS, Klei L, et al. Identification of common variants influencing risk of the tauopathy Progressive Supranuclear Palsy. Nat Genet. 2011 Jun 19;43(7):699–705.

21. Pickering-Brown SM, Rollinson S, Du Plessis D, Morrison KE, Varma A, Richardson AMT, et al. Frequency and clinical characteristics of progranulin mutation carriers in the

Manchester frontotemporal lobar degeneration cohort: comparison with patients with MAPT and no known mutations. Brain. 2008 Mar 1;131(3):721–31.

22. Rohrer JD, Warren JD. Phenotypic signatures of genetic frontotemporal dementia. Curr Opin Neurol. 2011 Dec;24(6):542.

23. Van Langenhove T, van der Zee J, Gijselinck I, Engelborghs S, Vandenberghe R, Vandenbulcke M, et al. Distinct Clinical Characteristics of C9orf72 Expansion Carriers Compared With GRN, MAPT, and Nonmutation Carriers in a Flanders-Belgian FTLD Cohort. JAMA Neurol. 2013 Mar 1;70(3):365–73.

24. Van Mossevelde S, van der Zee J, Gijselinck I, Engelborghs S, Sieben A, Van Langenhove T, et al. Clinical features of TBK1 carriers compared with C9orf72, GRN and non-mutation carriers in a Belgian cohort. Brain. 2016 Feb 1;139(2):452–67.

25. Tipton PW, Deutschlaender AB, Savica R, Heckman MG, Brushaber DE, Dickerson BC, et al. Differences in Motor Features of C9orf72, MAPT, or GRN Variant Carriers With Familial Frontotemporal Lobar Degeneration. Neurology. 2022 Sep 13;99(11):e1154–67.

26. Dabin LC, Guntoro F, Campbell T, Bélicard T, Smith AR, Smith RG, et al. Altered DNA methylation profiles in blood from patients with sporadic Creutzfeldt–Jakob disease. Acta Neuropathol (Berl). 2020;140(6):863–79.

27. Bettencourt C, Foti SC, Miki Y, Botia J, Chatterjee A, Warner TT, et al. White matter DNA methylation profiling reveals deregulation of HIP1, LMAN2, MOBP, and other loci in multiple system atrophy. Acta Neuropathol (Berl). 2020 Jan 1;139(1):135–56.

28. Murthy M, Fodder K, Miki Y, Rambarack N, De Pablo Fernandez E, Pihlstrøm L, et al. DNA methylation patterns in the frontal lobe white matter of multiple system atrophy, Parkinson's disease, and progressive supranuclear palsy: a cross-comparative investigation. Acta Neuropathol (Berl). 2024 Jul 12;148(1):4.

29. Bell CG. Epigenomic insights into common human disease pathology. Cell Mol Life Sci CMLS. 2024 Apr 11;81(1):178.

30. Taskesen E, Mishra A, van der Sluis S, Ferrari R, Veldink JH, van Es MA, et al. Susceptible genes and disease mechanisms identified in frontotemporal dementia and frontotemporal dementia with Amyotrophic Lateral Sclerosis by DNA-methylation and GWAS. Sci Rep. 2017 Aug 21;7(1):8899.

31. Xi Z, Zhang M, Bruni AC, Maletta RG, Colao R, Fratta P, et al. The C9orf72 repeat expansion itself is methylated in ALS and FTLD patients. Acta Neuropathol (Berl). 2015 May 1;129(5):715–27.

32. Galimberti D, D'Addario C, Dell'Osso B, Fenoglio C, Marcone A, Cerami C, et al. Progranulin gene (GRN) promoter methylation is increased in patients with sporadic frontotemporal lobar degeneration. Neurol Sci. 2013 Jun 1;34(6):899–903.

33. Banzhaf-Strathmann J, Claus R, Mücke O, Rentzsch K, van der Zee J, Engelborghs S, et al. Promoter DNA methylation regulates progranulin expression and is altered in FTLD. Acta Neuropathol Commun. 2013 May 13;1:16.

34. Huin V, Deramecourt V, Caparros-Lefebvre D, Maurage CA, Duyckaerts C, Kovari E, et al. The MAPT gene is differentially methylated in the progressive supranuclear palsy brain. Mov Disord Off J Mov Disord Soc. 2016 Dec;31(12):1883–90.

35. Fodder K, Murthy M, Rizzu P, Toomey CE, Hasan R, Humphrey J, et al. Brain DNA methylomic analysis of frontotemporal lobar degeneration reveals OTUD4 in shared dysregulated signatures across pathological subtypes. Acta Neuropathol (Berl). 2023;146(1):77–95.

36. Field AE, Robertson NA, Wang T, Havas A, Ideker T, Adams PD. DNA Methylation Clocks in Aging: Categories, Causes, and Consequences. Mol Cell. 2018 Sep 20;71(6):882–95.

37. Murthy M, Rizzu P, Heutink P, Mill J, Lashley T, Bettencourt C. Epigenetic Age Acceleration in Frontotemporal Lobar Degeneration: A Comprehensive Analysis in the Blood and Brain. Cells. 2023 Jul 24;12(14):1922.

38. Delgado-Morales R, Esteller M. Opening up the DNA methylome of dementia. Mol Psychiatry. 2017 Apr;22(4):485–96.

39. Menden K, Francescatto M, Nyima T, Blauwendraat C, Dhingra A, Castillo-Lizardo M, et al. A multi-omics dataset for the analysis of frontotemporal dementia genetic subtypes. Sci Data. 2023 Dec 1;10:849.

40. Weber A, Schwarz SC, Tost J, Trümbach D, Winter P, Busato F, et al. Epigenome-wide DNA methylation profiling in Progressive Supranuclear Palsy reveals major changes at DLX1. Nat Commun. 2018 Jul 26;9:2929.

41. Aryee MJ, Jaffe AE, Corrada-Bravo H, Ladd-Acosta C, Feinberg AP, Hansen KD, et al. Minfi: a flexible and comprehensive Bioconductor package for the analysis of Infinium DNA methylation microarrays. Bioinformatics. 2014 Jan 28;30(10):1363.

42. Pidsley R, Wong CCY, Volta M, Lunnon K, Mill J, Schalkwyk LC. A data-driven approach to preprocessing Illumina 450K methylation array data. BMC Genomics. 2013 May 1;14:293.

43. Tian Y, Morris TJ, Webster AP, Yang Z, Beck S, Feber A, et al. ChAMP: updated methylation analysis pipeline for Illumina BeadChips. Bioinformatics. 2017 Aug 14;33(24):3982.

44. Du P, Zhang X, Huang CC, Jafari N, Kibbe WA, Hou L, et al. Comparison of Beta-value and M-value methods for quantifying methylation levels by microarray analysis. BMC Bioinformatics. 2010 Nov 30;11:587.

45. Hasan R, Humphrey J, Bettencourt C, Newcombe J, Consortium NA, Lashley T, et al. Transcriptomic analysis of frontotemporal lobar degeneration with TDP-43 pathology reveals cellular alterations across multiple brain regions. Acta Neuropathol (Berl). 2021 Dec 28;143(3):383.

46. Ritchie ME, Phipson B, Wu D, Hu Y, Law CW, Shi W, et al. limma powers differential expression analyses for RNA-sequencing and microarray studies. Nucleic Acids Res. 2015 Apr 20;43(7):e47.

47. Wang X, Allen M, Reddy JS, Carrasquillo MM, Asmann YW, Funk C, et al. Conserved Architecture of Brain Transcriptome Changes between Alzheimer's Disease and Progressive Supranuclear Palsy in Pathologically Affected and Unaffected Regions

[Internet]. bioRxiv; 2021 [cited 2024 Nov 15]. p. 2021.01.18.426999. Available from: https://www.biorxiv.org/content/10.1101/2021.01.18.426999v1

48. Jones PA. The DNA methylation paradox. Trends Genet. 1999 Jan 1;15(1):34–7.

49. Jones PA. Functions of DNA methylation: islands, start sites, gene bodies and beyond. Nat Rev Genet. 2012 Jul;13(7):484–92.

50. Maunakea AK, Nagarajan RP, Bilenky M, Ballinger TJ, D'Souza C, Fouse SD, et al. Conserved Role of Intragenic DNA Methylation in Regulating Alternative Promoters. Nature. 2010 Jul 8;466(7303):253.

51. Suzuki MM, Bird A. DNA methylation landscapes: provocative insights from epigenomics. Nat Rev Genet. 2008 Jun;9(6):465–76.

52. Flanagan JM, Wild L. An epigenetic role for noncoding RNAs and intragenic DNA methylation. Genome Biol. 2007 Jun 27;8(6):307.

53. Shann YJ, Cheng C, Chiao CH, Chen DT, Li PH, Hsu MT. Genome-wide mapping and characterization of hypomethylated sites in human tissues and breast cancer cell lines. Genome Res. 2008 May;18(5):791.

54. McGuire MH, Herbrich SM, Dasari SK, Wu SY, Wang Y, Rupaimoole R, et al. Pan-cancer genomic analysis links 3'UTR DNA methylation with increased gene expression in T cells. EBioMedicine. 2019 May;43:127–37.

55. Mishra NK, Guda C. Genome-wide DNA methylation analysis reveals molecular subtypes of pancreatic cancer. Oncotarget. 2017 Apr 25;8(17):28990–9012.

56. Ferrari R, Ryten M, Simone R, Trabzuni D, Nicolaou N, Hondhamuni G, et al. Assessment of common variability and expression quantitative trait loci for genome-wide associations for progressive supranuclear palsy. Neurobiol Aging. 2014 Jun;35(6):1514.e1-12.

57. Liu QY, Yu JT, Miao D, Ma XY, Wang HF, Wang W, et al. An exploratory study on STX6, MOBP, MAPT, and EIF2AK3 and late-onset Alzheimer's disease. Neurobiol Aging. 2013 May;34(5):1519.e13-17.

58. Farrell K, Humphrey J, Chang T, Zhao Y, Leung YY, Kuksa PP, et al. Genetic, transcriptomic, histological, and biochemical analysis of progressive supranuclear palsy implicates glial activation and novel risk genes. Nat Commun. 2024 Sep 9;15(1):7880.

59. Jung JJ, Inamdar SM, Tiwari A, Choudhury A. Regulation of intracellular membrane trafficking and cell dynamics by syntaxin-6. Biosci Rep. 2012 Aug 1;32(Pt 4):383–91.

60. Bock JB, Lin RC, Scheller RH. A New Syntaxin Family Member Implicated in Targeting of Intracellular Transport Vesicles *. J Biol Chem. 1996 Jul 26;271(30):17961–5.

61. Wingo AP, Liu Y, Gerasimov ES, Gockley J, Logsdon BA, Duong DM, et al. Integrating human brain proteomes with genome-wide association data implicates new proteins in Alzheimer's disease pathogenesis. Nat Genet. 2021 Feb;53(2):143–6.

62. Yu L, Boyle PA, Wingo AP, Yang J, Wang T, Buchman AS, et al. Neuropathologic Correlates of Human Cortical Proteins in Alzheimer Disease and Related Dementias. Neurology. 2022 Mar 8;98(10):e1031–9.

63. Jones E, Hill E, Linehan J, Nazari T, Caulder A, Codner GF, et al. Characterisation and prion transmission study in mice with genetic reduction of sporadic Creutzfeldt-Jakob disease risk gene *Stx6*. Neurobiol Dis. 2024 Jan 1;190:106363.

64. Hill EA. The Role of Syntaxin-6 in Prion Diseases and Tauopathies [Internet] [Doctoral]. Doctoral thesis, UCL (University College London). UCL (University College London); 2024 [cited 2025 Jan 20]. p. 1–1. Available from: https://discovery.ucl.ac.uk/id/eprint/10200063/

65. Küçükali F, Hill E, Watzeels T, Hummerich H, Campbell T, Darwent L, et al. Multiomic analyses direct hypotheses for Creutzfeldt-Jakob disease risk genes. Brain. 2025 Jan 27;awaf032.

66. Fodder K, de Silva R, Warner TT, Bettencourt C. The contribution of DNA methylation to the (dys)function of oligodendroglia in neurodegeneration. Acta Neuropathol Commun. 2023 Jun 29;11(1):106.

67. Forrest SL, Kril JJ, Halliday GM. Cellular and regional vulnerability in frontotemporal tauopathies. Acta Neuropathol (Berl). 2019 Nov 1;138(5):705–27.

68. Gao YL, Wang N, Sun FR, Cao XP, Zhang W, Yu JT. Tau in neurodegenerative disease. Ann Transl Med. 2018 May;6(10):175.

69. Lee WS, Tan DC, Deng Y, vanHummel A, Ippati S, Stevens C, et al. Syntaxins 6 and 8 facilitate tau into secretory pathways. Biochem J. 2021 Apr 16;478(7):1471.

70. Ito S ichi, Tanaka Y. Evaluation of LC3-II Release via Extracellular Vesicles in Relation to the Accumulation of Intracellular LC3-positive Vesicles. J Vis Exp JoVE. 2024 Oct 18;(212):e67385.

71. Tanaka Y, Ito S ichi, Suzuki G. TDP-43 Secretion via Extracellular Vesicles Is Regulated by Macroautophagy. Autophagy Rep. 2024 Dec 31;3(1):2291250.

72. Dingjan I, Linders PTA, Verboogen DRJ, Revelo NH, ter Beest M, van den Bogaart G. Endosomal and Phagosomal SNAREs. Physiol Rev. 2018 Jul;98(3):1465–92.

73. Spillantini MG, Goedert M. Tau pathology and neurodegeneration. Lancet Neurol. 2013 Jun 1;12(6):609–22.

74. Corsi A, Bombieri C, Valenti MT, Romanelli MG. Tau Isoforms: Gaining Insight into MAPT Alternative Splicing. Int J Mol Sci. 2022 Dec 6;23(23):15383.

75. Ressler HW, Humphrey J, Vialle RA, Babrowicz B, Kandoi S, Raj T, et al. MAPT haplotype-associated transcriptomic changes in progressive supranuclear palsy. Acta Neuropathol Commun. 2024 Aug 17;12(1):135.

76. Caillet-Boudin ML, Buée L, Sergeant N, Lefebvre B. Regulation of human MAPT gene expression. Mol Neurodegener. 2015 Jul 14;10(1):28.

77. Baker M, Litvan I, Houlden H, Adamson J, Dickson D, Perez-Tur J, et al. Association of an Extended Haplotype in the Tau Gene with Progressive Supranuclear Palsy. Hum Mol Genet. 1999 Apr 1;8(4):711–5.

78. Boettger LM, Handsaker RE, Zody MC, McCarroll SA. Structural haplotypes and recent evolution of the human 17q21.31 region. Nat Genet. 2012 Jul 1;44(8):881–5.

79. Andreadis A, Brown WM, Kosik KS. Structure and novel exons of the human tau gene. Biochemistry. 1992 Nov 3;31(43):10626–33.

80. Caffrey TM, Wade-Martins R. Functional MAPT haplotypes: Bridging the gap between genotype and neuropathology. Neurobiol Dis. 2007 May 5;27(1):1.

81. Pedicone C, Weitzman SA, Renton AE, Goate AM. Unraveling the complex role of MAPT-containing H1 and H2 haplotypes in neurodegenerative diseases. Mol Neurodegener. 2024 May 29;19(1):43.

82. Valentino RR, Scotton WJ, Roemer SF, Lashley T, Heckman MG, Shoai M, et al. MAPT H2 haplotype and risk of Pick's disease in the Pick's disease International Consortium: a genetic association study. Lancet Neurol. 2024 May 1;23(5):487–99.

83. Ghidoni R, Signorini S, Barbiero L, Sina E, Cominelli P, Villa A, et al. The H2 MAPT haplotype is associated with familial frontotemporal dementia. Neurobiol Dis. 2006 May;22(2):357–62.

84. Li Y, Chen JA, Sears RL, Gao F, Klein ED, Karydas A, et al. An Epigenetic Signature in Peripheral Blood Associated with the Haplotype on 17q21.31, a Risk Factor for Neurodegenerative Tauopathy. PLOS Genet. 2014 Mar 6;10(3):e1004211.

85. Iwata A, Nagata K, Hatsuta H, Takuma H, Bundo M, Iwamoto K, et al. Altered CpG methylation in sporadic Alzheimer's disease is associated with APP and MAPT dysregulation. Hum Mol Genet. 2014 Feb 1;23(3):648–56.

86. Coupland KG, Mellick GD, Silburn PA, Mather K, Armstrong NJ, Sachdev PS, et al. DNA Methylation of MAPT Gene in Parkinson's Disease Cohorts and Modulation by Vitamin E In Vitro. Mov Disord Off J Mov Disord Soc. 2013 Dec 27;29(13):1606.

87. Barrachina M, Ferrer I. DNA methylation of Alzheimer disease and tauopathy-related genes in postmortem brain. J Neuropathol Exp Neurol. 2009 Aug;68(8):880–91.

88. Steri M, Idda ML, Whalen MB, Orrù V. Genetic Variants in mRNA Untranslated Regions. Wiley Interdiscip Rev RNA. 2018 Mar 26;9(4):e1474.

89. Mignone F, Gissi C, Liuni S, Pesole G. Untranslated regions of mRNAs. Genome Biol. 2002 Feb 28;3(3):reviews0004.1.

90. Huin V, Buée L, Behal H, Labreuche J, Sablonnière B, Dhaenens CM. Alternative promoter usage generates novel shorter MAPT mRNA transcripts in Alzheimer's disease and progressive supranuclear palsy brains. Sci Rep. 2017 Oct 3;7:12589.

91. Boland S, Swarup S, Ambaw YA, Malia PC, Richards RC, Fischer AW, et al. Deficiency of the frontotemporal dementia gene GRN results in gangliosidosis. Nat Commun. 2022 Oct 7;13(1):5924.

92. Cruts M, Gijselinck I, van der Zee J, Engelborghs S, Wils H, Pirici D, et al. Null mutations in progranulin cause ubiquitin-positive frontotemporal dementia linked to chromosome 17q21. Nature. 2006 Aug 24;442(7105):920–4.

93. Ward ME, Chen R, Huang HY, Ludwig C, Telpoukhovskaia M, Taubes A, et al. Individuals with progranulin haploinsufficiency exhibit features of neuronal ceroid lipofuscinosis. Sci Transl Med. 2017 Apr 12;9(385):eaah5642.

94. Kao AW, McKay A, Singh PP, Brunet A, Huang EJ. Progranulin, lysosomal regulation and neurodegenerative disease. Nat Rev Neurosci. 2017 Jun;18(6):325–33.

95. Paushter DH, Du H, Feng T, Hu F. The lysosomal function of progranulin, a guardian against neurodegeneration. Acta Neuropathol (Berl). 2018 Jul;136(1):1–17.

96. Rhinn H, Tatton N, McCaughey S, Kurnellas M, Rosenthal A. Progranulin as a therapeutic target in neurodegenerative diseases. Trends Pharmacol Sci. 2022 Aug 1;43(8):641–52.

97. Van Damme P, Van Hoecke A, Lambrechts D, Vanacker P, Bogaert E, van Swieten J, et al. Progranulin functions as a neurotrophic factor to regulate neurite outgrowth and enhance neuronal survival. J Cell Biol. 2008 Apr 7;181(1):37–41.

98. Kuang L, Hashimoto K, Huang EJ, Gentry MS, Zhu H. Frontotemporal dementia non-sense mutation of progranulin rescued by aminoglycosides. Hum Mol Genet. 2020 Mar 13;29(4):624–34.

99. Davis SE, Cook AK, Hall JA, Voskobiynyk Y, Carullo NV, Boyle NR, et al. Patients with sporadic FTLD exhibit similar increases in lysosomal proteins and storage material as patients with FTD due to GRN mutations. Acta Neuropathol Commun. 2023 Apr 28;11(1):70.

100. Rademakers R, Eriksen JL, Baker M, Robinson T, Ahmed Z, Lincoln SJ, et al. Common variation in the miR-659 binding-site of GRN is a major risk factor for TDP43-positive frontotemporal dementia. Hum Mol Genet. 2008 Dec 1;17(23):3631–42.

101. Beck J, Rohrer JD, Campbell T, Isaacs A, Morrison KE, Goodall EF, et al. A distinct clinical, neuropsychological and radiological phenotype is associated with progranulin gene mutations in a large UK series. Brain J Neurol. 2008 Mar;131(Pt 3):706–20.

102. Rohrer JD, Ridgway GR, Modat M, Ourselin S, Mead S, Fox NC, et al. Distinct profiles of brain atrophy in frontotemporal lobar degeneration caused by progranulin and tau mutations. NeuroImage. 2010 Nov 15;53(3):1070–6.

103. Gendron TF, Petrucelli L. Disease Mechanisms of C9ORF72 Repeat Expansions. Cold Spring Harb Perspect Med. 2018 Apr;8(4):a024224.

104. Braems E, Swinnen B, Van Den Bosch L. C9orf72 loss-of-function: a trivial, stand-alone or additive mechanism in C9 ALS/FTD? Acta Neuropathol (Berl). 2020;140(5):625–43.

105. Lee YB, Chen HJ, Peres JN, Gomez-Deza J, Attig J, Štalekar M, et al. Hexanucleotide Repeats in ALS/FTD Form Length-Dependent RNA Foci, Sequester RNA Binding Proteins, and Are Neurotoxic. Cell Rep. 2013 Dec 12;5(5):1178–86.

106. Mori K, Arzberger T, Grässer FA, Gijselinck I, May S, Rentzsch K, et al. Bidirectional transcripts of the expanded C9orf72 hexanucleotide repeat are translated into aggregating dipeptide repeat proteins. Acta Neuropathol (Berl). 2013 Dec 1;126(6):881–93.

107. Zu T, Liu Y, Bañez-Coronel M, Reid T, Pletnikova O, Lewis J, et al. RAN proteins and RNA foci from antisense transcripts in C9ORF72 ALS and frontotemporal dementia. Proc Natl Acad Sci. 2013 Dec 17;110(51):E4968–77.

108. Mizielinska S, Lashley T, Norona FE, Clayton EL, Ridler CE, Fratta P, et al. C9orf72 frontotemporal lobar degeneration is characterised by frequent neuronal sense and antisense RNA foci. Acta Neuropathol (Berl). 2013 Dec 1;126(6):845–57.

109. Gendron TF, Bieniek KF, Zhang YJ, Jansen-West K, Ash PEA, Caulfield T, et al. Antisense transcripts of the expanded C9ORF72 hexanucleotide repeat form nuclear RNA foci and undergo repeat-associated non-ATG translation in c9FTD/ALS. Acta Neuropathol (Berl). 2013 Dec 1;126(6):829–44.

110. Gitler AD, Tsuiji H. There has been an awakening: Emerging mechanisms of *C9orf72* mutations in FTD/ALS. Brain Res. 2016 Sep 15;1647:19–29.

111. Smeyers J, Banchi EG, Latouche M. C9ORF72: What It Is, What It Does, and Why It Matters. Front Cell Neurosci. 2021 May 5;15:661447.

112. Pang W, Hu F. Cellular and physiological functions of C9ORF72 and implications for ALS/FTD. J Neurochem. 2021 May;157(3):334–50.

113. Rizzu P, Blauwendraat C, Heetveld S, Lynes EM, Castillo-Lizardo M, Dhingra A, et al. C9orf72 is differentially expressed in the central nervous system and myeloid cells and consistently reduced in C9orf72, MAPT and GRN mutation carriers. Acta Neuropathol Commun. 2016 Apr 14;4(1):37.

114. Fratta P, Poulter M, Lashley T, Rohrer JD, Polke JM, Beck J, et al. Homozygosity for the C9orf72 GGGGCC repeat expansion in frontotemporal dementia. Acta Neuropathol (Berl). 2013 Sep 1;126(3):401–9.

115. Liu EY, Russ J, Wu K, Neal D, Suh E, McNally AG, et al. C9orf72 hypermethylation protects against repeat expansion-associated pathology in ALS/FTD. Acta Neuropathol (Berl). 2014 Oct;128(4):525–41.